NASA TN D-1624

TECHNICAL NOTE

D-1624

INVESTIGATION OF THE SKID-ROCKER LANDING CHARACTERISTICS OF SPACECRAFT MODELS

By Sandy M. Stubbs

Langley Research Center
Langley Station, Hampton, Va.

NATIONAL AERONAUTICS AND SPACE ADMINISTRATION
WASHINGTON
April 1963

NATIONAL AERONAUTICS AND SPACE ADMINISTRATION

TECHNICAL NOTE D-1624

INVESTIGATION OF THE SKID-ROCKER LANDING CHARACTERISTICS OF SPACECRAFT MODELS

By Sandy M. Stubbs

SUMMARY

An experimental investigation was made of the skid-rocker landing characteristics of two dynamic models of proposed reentry vehicles. A "belly-landing" technique in which the vehicle was caused to skid and rock on its curved lower surface (heat shield) in order to convert sinking-speed energy into angular energy was investigated on a hard-surface runway for speed ranges that might be encountered with the use of a paraglider letdown system. Several landings were also made in calm water. Landing motions and acceleration data were obtained over a range of landing attitudes, horizontal velocities, and vertical velocities. Turnover stability limits for various center-of-gravity locations were determined for hard-surface landings. A brief experimental study was made of the effect of a small edge-mounted shock absorber on accelerations and rocking motions.

Acceptable hard-surface landings could be made with all the configurations at landing attitudes between -30° and 10°. For bodies of short length and high center of gravity, the possibility of converting sinking-speed energy into angular energy was substantially limited because of the instability (turnover) at landing attitudes greater than 10°. The landings resulted in maximum normal and angular accelerations of 15g and 70 radians per second^2, respectively, over a range of landing conditions. Water landings were satisfactory at horizontal landing velocities of 50 and 80 feet per second. Landings at 130 feet per second resulted in violent rebound at first impact followed by random impacts and high accelerations.

INTRODUCTION

Earth-landing requirements of multimanned lunar-mission vehicles indicate a need for spacecraft to have the capability of landing on land or sea. A compatible system having little weight directly chargeable to the landing system might be possible with the use of the "belly-landing" concept discussed in reference 1. The belly-landing or skid-rocker system was previously investigated over a range of landing speeds and attitudes associated with fixed-wing aircraft by using a lenticular-shaped lifting body having horizontal fins for control. (See ref. 2.) The present investigation of this landing concept includes landing speeds and

attitudes considered feasible for flared paraglider landings of low-lift reentry spacecraft applicable to the lunar mission.

The purpose of this investigation was to determine the accelerations and motions that would be encountered during landings of two proposed space vehicles using the curved lower surface (heat shield) of the vehicles as a skid-rocker which converted sinking-speed energy into angular energy in pitch (rocking oscillation). The landings were made with free-launched dynamic models on a hard-surface runway and on water. Turnover stability tests were made with various ratios of center-of-gravity height to body diameter. It was assumed for the investigation that the paraglider would be released at vehicle touchdown.

DESCRIPTION OF MODELS

The general arrangement of the two basic models and related lower-surface (heat shield) geometry are shown in figures 1 and 2. Figure 1 shows the 1/8-scale dynamic model consisting of a frustum of a cone with three interchangeable lower-surface shapes, which are designated configurations A, B, and C. Figure 2 shows the 1/10-scale model having a 30° conical upper surface and a spheroidal lower surface, designated configuration D. Photographs of configurations B and D are shown as figures 3 and 4, respectively. Figure 5 shows a small shock absorber installed near the maximum diameter (outer edge) of configuration D. Additional information about the configurations is given in table I.

The models were constructed of balsa and hardwood cores covered with plastic and fiber glass. The lower surface of configuration A simulated a 384-inch-radius spherical heat shield with a ratio of center-of-gravity height to body diameter of 0.2. Configuration B had for its lower surface a hyperboloid of revolution designed to reduce maximum acceleration, in comparison with configuration A, during rocking motion. The ratio of center-of-gravity height to body diameter was 0.22. Configuration C utilized the same lower-surface shape as configuration B; however, the lower surface was extended to a greater diameter. The ratio of center-of-gravity height to diameter was 0.2. The lower surface of configuration D simulated a 187-inch-radius spherical heat shield. The ratio of center-of-gravity height to diameter was 0.25, and the center of gravity of this configuration was offset forward 5.5 inches (full scale) from the vertical center line. The small shock absorber used with configuration D was a soft aluminum plate installed in such a manner that a resisting force and stroke was provided for shock absorption at initial impact.

APPARATUS AND PROCEDURE

The investigation was conducted by launching the model as a free body with the free-launch apparatus of the Langley impact structures facility. Landings were made on a hard-surface runway with the monorail equipment shown in figure 6(a). The catapult apparatus shown in figure 6(b) was used for landings in fresh water. The hard-surface runway was constructed of heavy wood decking covered with 1/2-inch plywood and supported just above the water surface on

adjustable steel scaffolding mounted on the bottom of a tank of water. The landing surface was 8 feet wide and approximately 100 feet long.

The orientation of acceleration axes, attitudes, and flight paths investigated are shown in figure 7. Hard-surface landings were made at contact attitudes of $\pm 10^{\circ}$, $+20^{\circ}$, and $\pm 30^{\circ}$; at horizontal velocities of 30, 80, and 130 feet per second; and at vertical velocities of 5 and 10 feet per second. (All values given herein are full scale.) These landing parameters simulate conditions expected at touchdown after paraglider flare-out. Configurations A, B, C, and D were landed at most of the preceding conditions. The sliding coefficient of friction between the plywood runway and the fiber-glass model was approximately 0.35 to 0.45 during hard-surface landings.

A brief investigation was also made with configuration C to determine the effect of center-of-gravity height on stability. Ratios of center-of-gravity height to body diameter of 0.20, 0.25, 0.30, and 0.40 were investigated. In order to obtain these ratios, it was necessary to increase the weight of the model and the moments of inertia. Table II shows these changes. Landings were made at contact attitudes of 0°, $\pm 10^{\circ}$, $\pm 20^{\circ}$, -30°, -45°, and -52°, at horizontal velocities of 30 and 80 feet per second, and at a vertical velocity of 10 feet per second.

A limited number of landings were made with configuration D with the use of a small shock absorber (fig. 5) to dissipate energy at the point of initial contact and initiate rocking motion. Landings were made at an attitude of 33° in order to make initial contact on the shock absorber. The effect on acceleration and motion was determined for a horizontal landing velocity of 80 feet per second and a vertical velocity of 10 feet per second.

Calm-water landings were made with configuration C. The landing attitudes tested were 20° and 0°; the horizontal velocities were 50, 80, and 130 feet per second; and the vertical velocity was 5 feet per second.

Normal, longitudinal, and angular accelerations at the vehicle center of gravity were measured by strain-gage accelerometers rigidly mounted to the model structure. Normal and longitudinal accelerations were measured with 50g and 25g accelerometers, respectively, and angular acceleration was measured with a pair of matched 50g accelerometers. The natural frequency was about 630 and 350 cycles per second for the separate 50g and 25g accelerometers, respectively, and about 310 cycles per second for the matched pair of 50g accelerometers. The accelerometers were damped to 65 percent of critical damping. The response of the recording galvanometers was flat to about 135 cycles per second for all accelerometers. A trailing cable, supported by an overhead guide wire, was used to transmit accelerometer signals to an oscillograph recorder. Motion-picture cameras were located at the side of the runway and also at the end of the runway to record general behavior.

RESULTS AND DISCUSSION

A short motion-picture film supplement of typical hard-surface and water landings is available on loan. A request card form and a description of the film will be found at the back of this paper, on the page immediately preceding the abstract and index pages.

All data presented are converted to full-scale values by use of the scale relations given in table III. Acceleration data for the landing conditions investigated are given in tables IV and V. Data plots that show trends and ranges are presented in subsequent sections.

Hard-Surface Landings

General.- Sequence photographs of typical landings of configuration C on the hard-surface runway are shown in figure 8. The general behavior for most hard-surface landings was characterized by approach at the landing attitude, touchdown, transition to angular oscillation (rocking) along the lower surface of the vehicle, and the slide-out or turnover. The model initially pitched nose down for positive landing attitudes and oscillated in pitch about the friction angle. The friction angle for configuration C is approximately -12°. (The friction angle is the attitude angle at which the model would slide without oscillation in pitch.) The main factors governing the friction angle are friction forces, lower-surface geometry, and center-of-gravity location. For negative landing attitudes greater than the friction angle (-13° to -30°), the model pitched nose up after initial contact. The computed friction angles for configurations A, B, and D are -2°, -12°, and -5°, respectively.

Typical oscillograph records of acceleration during the hard-surface landings are shown in figure 9. High-frequency hash, caused by irregularities between stiff sliding surfaces (model and runway) and by model vibrations, was faired as shown by the dashed line in figure 9. The acceleration values obtained from the faired line are given in table IV. During the skid-rocker landing, initial contact occurred at time t_0. (See top part of fig. 9.) The ground-contact point moved forward as the vehicle rocked forward and a maximum acceleration occurred at time t_1 as the contact point passed below the center of gravity (approximately 0° attitude) and the vertical motion (fall) of the center of gravity was stopped. The ground-contact point continued to move forward as the vehicle pitched to a nose-low attitude. When the resultant ground reaction moved far enough forward to overcome the angular momentum, the rocking motion was reversed. As the vehicle rocked back through 0° attitude, another acceleration pulse occurred at time t_2. Subsequent rocking oscillations (not shown in fig. 9) generally had lower accelerations. For the purpose of this investigation, the initial acceleration peak that occurred at touchdown was not considered since a small load-alleviation system of crushing or yielding metal or the normal flexibility of the vehicle could be used to minimize this acceleration and to initiate the rocking motion. (See discussion on the effect of the shock absorber that follows in this report and in refs. 1 and 2.)

Effect of landing velocity.- The effects of vertical and horizontal velocity on normal acceleration for the four configurations tested are shown in figure 10. The shaded data points on figure 10 indicate that the model turned over. Acceleration data given in this figure were recorded during the first rocking motion and prior to turnover. The vertical velocity of 10 feet per second resulted in a normal acceleration of approximately twice that obtained at a vertical velocity of 5 feet per second. Horizontal velocity had little effect on acceleration.

Effect of lower-surface geometry.- Also shown in figure 10 are the variations in normal acceleration due to differences in the configuration lower-surface geometry. Configuration A was found to be very stable because of a relatively flat lower surface; however, acceleration was high and it was felt that the accelerations could be reduced considerably by changing the lower-surface geometry. Use of configuration B which has greater curvature than configuration A resulted in about a 50-percent reduction in the normal accelerations, but configuration B was less stable than configuration A. Configuration C which had a greater diameter than configuration B proved to have acceleration characteristics similar to configuration B and better stability. Configuration D which has a lower-surface curvature between that of configuration A and configurations B and C was tested only briefly. The limited data available indicate the landing accelerations and behavior were about the same as those of configurations B and C.

Effect of landing attitude.- Variation in maximum normal acceleration due to landing attitude is shown in figure 11 and table IV. There was a tendency for increased normal acceleration as the landing attitude was changed from -30° to 30°. The maximum normal and angular accelerations for the first rocking motion occurred with configuration A and were about 15g and 70 radians per second^2, respectively, over the range of landing conditions investigated. The maximum normal accelerations for configurations B, C, and D were about 1g to 7g and maximum angular accelerations were about 50 radians per second^2.

Effect of shock absorber.- During landings at a vertical velocity of 10 feet per second, configuration D bounced several times following initial contact as shown by acceleration traces in figure 12(a). This bouncing was possibly due to the structural characteristics of the model. Adding the shock absorber (fig. 5) resulted in acceleration traces shown in figure 12(b). The shock absorber reduced rebound and acceleration at initial contact. Subsequent acceleration peaks due to bouncing were eliminated and a better transition and rocking motion were obtained. There was no noticeable effect on turnover characteristics at a landing attitude of 33°.

Energy conversion.- The conversion of sinking-speed energy into angular energy is best accomplished by landing so that the model contacts the landing surface at a point remote from the center of gravity. This stops the initial vertical motion at the contact point and causes rocking on the curved lower surface which gradually stops the vertical motion of the center of gravity as sinking-speed energy is converted into angular energy in pitch. Because of the geometry of the models, it was necessary to land at attitudes of 20° to 30° in order to have initial contact points at appreciable distances from the center of gravity. However, at these high positive attitudes, the models were unstable. Thus, for bodies of short length and high center of gravity, the possibilities of converting sinking-speed energy into angular energy were substantially limited.

Stability.- An investigation made with configuration C to determine the effect of center-of-gravity height on model turnover stability gave the experimental results shown in figure 13. Also shown are computed stability limits from reference 3. In general, the hard-surface landing stability characteristics of the configurations tested were good over a small range of positive landing attitudes and a fairly wide range of negative attitudes.

Water Landings

Sequence photographs of typical landings of configuration C at an attitude of 20° in calm water are shown in figure 14. Acceleration data are presented in table V. Typical oscillograph records of accelerations during landings in calm water are shown in figure 15. At a horizontal velocity of 50 feet per second, motions and accelerations were slight. At 80 feet per second, three distinct acceleration peaks occurred and the model skipped clear of the water twice. At a horizontal velocity of 130 feet per second, the model skimmed along the water surface and pitched down to a low attitude with little reduction in velocity. As a result, a large restoring force was generated by the rapid increase of lower-surface wetted area. This force and the body shape caused an abrupt change in attitude along with large and erratic rebounds. The subsequent impacts frequently occurred at highly yawed, highly rolled, tail first, or inverted contact attitudes. Overall behavior was very similar but more pronounced during landings at an initial attitude of 0°. Because of this trend, negative attitudes were not tested. As shown in figure 16, accelerations increased with increased landing speed and landings made at a landing attitude of 20° resulted in lower accelerations than those made at an attitude of 0°. Maximum landing accelerations on water were approximately 2g to 10g normal and 14 to 74 radians per second^2 angular

CONCLUDING REMARKS

Hard-surface landing characteristics of several spacecraft configurations simulating paraglider letdown and using curved lower surfaces (heat shields) as skid-rockers were acceptable for landing attitudes between -30° and 10°. Landings made at attitudes greater than 10° were unstable. For bodies having short length and high center of gravity, the possibilities of converting sinking-speed energy into angular energy were substantially limited. The maximum normal and angular accelerations, for all configurations tested, were 15g and 70 radians per second^2. The normal accelerations were reduced to 1g to 7g, and angular acceleration to about 50 radians per second^2 by using a configuration having a lower-surface geometry designed to give low constant-force loads during rocking motion. Horizontal velocity had little effect on accelerations, but an increase in vertical velocity from 5 to 10 feet per second approximately doubled the maximum normal acceleration.

A change in landing attitude from -30° to 30° resulted in an increase in acceleration. A small shock absorber installed at the point of initial contact had no appreciable effect on turnover stability; however, rocker action was improved and accelerations were reduced.

Landings in water at horizontal velocities of 50 to 80 feet per second were satisfactory. For water landings at a horizontal velocity of 130 feet per second, extreme attitude changes during rebound after initial impact made the attitude of subsequent impacts random. Maximum landing accelerations on water were approximately 2g to 10g normal and 14 to 74 radians per second^2 angular.

Langley Research Center,
National Aeronautics and Space Administration,
Langley Station, Hampton, Va., January 4, 1963.

REFERENCES

1. Mayo, Wilbur L.: Skid Landings of Airplanes on Rocker-Type Fuselages. NASA TN D-760, 1961.

2. Blanchard, Ulysse J.: Landing Characteristics of a Lenticular-Shaped Reentry Vehicle. NASA TN D-940, 1961.

3. Fralich, Robert W., and Kruszewski, Edwin T.: Theoretical Stability Analysis of Skid-Rocker Landings of Space Vehicles. NASA TN D-1625, 1963.

TABLE I.- PERTINENT CHARACTERISTICS OF SPACECRAFT MODELS

[All data are full scale]

	Configuration A	Configuration B	Configuration C	Configuration D
General:				
Model scale, λ	1/8	1/8	1/8	1/10
Gross weight, lb	7,000	7,000	7,000	7,000
Moment of inertia (approx.):				
Pitch, slug-ft^2	2,300	2,100	2,300	3,436
Roll, slug-ft^2	2,300	2,100	2,300	3,188
Yaw, slug-ft^2	3,085	3,420	3,560	3,732
Body:				
Height, ft	5.80	6.54	6.54	11.34
Diameter, ft	11.60	11.60	12.73	13.33
$\frac{\text{Center-of-gravity height}}{\text{Diameter ratio}}$	0.20	0.22	0.20	0.25

TABLE II.- CHARACTERISTICS OF CONFIGURATION C FOR STABILITY TESTS

[All data are full scale]

	Center-of-gravity height/Diameter ratio of -			
	0.20	0.25	0.30	0.40
Weight, lb	7,000	8,200	9,750	12,550
Moment of inertia (approx.):				
Pitch, slug-ft^2	2,300	3,050	3,470	5,640
Roll, slug-ft^2	2,300	3,050	3,470	5,640

TABLE III.- SCALE RELATIONSHIPS

[λ = Scale of model]

Quantity	Full scale	Scale factor	Model
Length	l	λ	λl
Area	A	λ^2	$\lambda^2 A$
Weight	W	λ^3	$\lambda^3 W$
Moment of inertia	I	λ^5	$\lambda^5 I$
Time	t	$\sqrt{\lambda}$	$\sqrt{\lambda} t$
Speed	V	$\sqrt{\lambda}$	$\sqrt{\lambda} v$
Linear acceleration	a	1	a
Angular acceleration	α	λ^{-1}	$\lambda^{-1}\alpha$
Force	F	λ^3	$\lambda^3 F$

TABLE IV.- MAXIMUM ACCELERATION DATA FOR HARD-SURFACE LANDINGS

(a) Configuration A

Vertical velocity, ft/sec	Horizontal velocity, ft/sec	Attitude, deg	Normal acceleration		Angular acceleration		Remarks
			1st rock, g	2d rock, g	1st rock, radians/sec^2	2d rock, radians/sec^2	
5	30	30	14.4		-56, 63		Turned over
5	30	30	12.6		-58, 54		Turned over
5	130	30	15.1		-35, 38		Turned over
5	130	30	12.6		-23, 49		Turned over
5	130	30	16.1		-31, 35		Turned over
5	130	30	14.4				Turned over
5	30	20	12.2		-36, 37		Turned over
5	30	20	12.7		-41, 24		Turned over
5	80	20	10.5	6.4	-92, 25	7, -34	
5	80	20	9.5	6.2	-39, 25	13, -33	
5	80	20	12.3	6.3	-51, 24	8, -40	
5	130	20	9.9	5.8	-24, 35	13, -28	
5	130	20	9.6	5.3	-34, 25	16, -27	
5	130	20	9.6	4.8	-23, 25	16, -23	
5	30	10	6.0	4.0	-31, 23	14, -22	
5	80	10		4.9		12, -20	
5	80	10	3.6	3.9	-29, 18	8, -19	
5	80	10	5.8	6.2	-44, 23	12, -20	
5	130	10	5.4	5.1	-35, 16	20, -14	
5	130	10	4.7	5.8	-37, 19	16, -18	
5	130	10	4.3	5.8	-34, 16	20, -16	
10	30	20	12.2		-49, 35		Turned over
10	80	20	4.9	6.2	31	6, -22	
10	80	20	6.0	6.2	44	10, -28	
10	80	20	2.2	4.9	32	17, -16	
10	130	20	10.0	5.3	-51, 24	22, -25	
10	130	20	12.5	7.2	-70, 33	16, -28	
10	130	20	3.5	4.5	-43, 23	15, -14	
10	30	10	8.9		-16, 23		Turned over
10	80	10	10.1	6.5	23	20, -16	
10	80	10	11.7	9.6	-34, 14	23, -20	
10	80	10	13.1	5.0	-47, 21	13, -21	
10	130	10	9.2	8.8	-35, 29	14, -23	
10	130	10	10.5	6.5	-27, 37	33, -28	
10	130	10	10.7	7.5	-48, 20	7, -24	

TABLE IV.- MAXIMUM ACCELERATION DATA FOR HARD-SURFACE LANDINGS - Continued

(b) Configuration B

Vertical velocity, ft/sec	Horizontal velocity, ft/sec	Attitude, deg	Normal acceleration		Angular acceleration		Remarks
			1st rock, g	2d rock, g	1st rock, radians/sec^2	2d rock, radians/sec^2	
5	30	30	2.8		-20, 32		Turned over
5	80	30	2.8		-21, 28		Turned over
5	130	30	2.6		-12, 28		Turned over
5	130	30	1.4		-9, 19		Turned over
5	30	20	3.1		-32, 40		Turned over
5	80	20	4.4	1.9	-37, 23	13, -11	Turned over
5	80	20	2.3	1.8	-37, 19	11, -12	Turned over
5	130	20	1.5	1.6	-28, 24	9, -12	Turned over
5	130	20	1.6	1.4	-29	10, -8	Turned over
5	130	20	1.6	1.4			
5	30	10	3.3	.8	-13, 17	9, -6	
5	30	10	3.2	.9	-15, 14	10, -6	
5	80	10	1.2	1.1	-19, 16	4, -9	
5	80	10	4.0	.9	-21, 18	6, -7	
5	130	10	3.0	.6	-13, 9	6, -6	
5	130	10	2.9	.6	-12, 10	6, -6	
5	30	-10	1.5	.3	3, -3	-3, 3	
5	80	-10	2.1	.4	-2	-2, 2	
5	130	-10	1.4	.9	3, -3	-3, 3	
5	30	-30	1.2		17, -7	-7, 8	
5	80	-30	3.6	1.1	28	-7, 8	
5	80	-30	1.6	1.1	16, -8	-6, 10	
5	130	-30	1.4	.6	14, -14	-11, 13	Turned over
5	130	-30	1.1	1.4	14, -14	-13, 11	
5	130	-30	1.0	2.0	18, -13	-9, 11	
10	30	20	7.3		-40, 25		Turned over
10	80	20	6.3		-40, 22		Turned over
10	30	10	7.2		42		Turned over
10	30	10	6.1		52		Turned over
10	30	10	5.7		26		Turned over
10	80	10	6.6	1.2	30	9, -10	Turned over
10	80	10	6.4	3.6	28	6, -14	Turned over
10	130	10	6.6	1.2	22	9, -7	
10	130	10	6.9	1.4	9	6, -7	
10	130	10	6.8	1.4	12	9, -7	Turned over
10	30	-10	6.8		-7		
10	80	-10	4.9	.7	1, -2	-1, 1	
10	130	-10	6.2	.6	7	-2, 4	
10	30	-30	7.7	1.1	-12	-6, 7	
10	80	-30	7.7	2.1	35, -11	-10, 37	Turned over
10	80	-30	5.2	2.3	33, -7	-10, 33	Turned over
10	130	-30	6.0	2.8	34, -14	-12, 32	Turned over

TABLE IV.- MAXIMUM ACCELERATION DATA FOR HARD-SURFACE LANDINGS - Continued

(c) Configuration C

Vertical velocity, ft/sec	Horizontal velocity, ft/sec	Attitude, deg	Normal acceleration		Angular acceleration		Remarks
			1st rock, g	2d rock, g	1st rock, radians/sec^2	2d rock, radians/sec^2	
5	30	30	4.4		-27, 50		Turned over
5	80	30	5.2		-27, 46		Turned over
5	80	30	4.9		-43, 46		Turned over
5	130	30	4.6	1.8	-29, 46	13, -12	
5	130	30	3.9	2.8	-25, 29	20, -12	
5	30	20	3.4		-31, 32		Turned over
5	80	20	2.7	2.8	-29, 36	11, -14	Turned over
5	80	20	2.5	1.7	-30, 37	25, -13	Turned over
5	130	20	3.2	1.1	-27, 31	24, -10	
5	130	20	1.8	1.5	-32, 29	26, -7	
5	30	10	3.5	.9	-17, 26	12, -9	
5	80	10	4.3	.7	-17, 8	9, -9	
5	80	10	3.4	.8	-19, 15	9, -7	
5	130	10	2.9	.9	-20, 14	6, -9	
5	130	10	3.5	1.3	-27, 12	7, -6	
5	30	-30	1.6	1.6	21, -7	-9, 26	
5	80	-30	1.6	.8	28	-8, 11	
5	80	-30	2.5	.7	22	-8, 11	
5	130	-30	2.9	1.1	25, -22	-6, 14	
5	130	-30	1.5	1.2	24, -25	-21, 20	
10	130	30	4.8		-15, 35		Turned over
10	130	30	4.5	2.7	-28, 28	12, -15	
10	30	20	8.1		-48, 57		Turned over
10	80	20	7.0		-44, 44		Turned over
10	80	20	7.8		-51, 44		Turned over
10	130	20	3.9	2.4	-23, 44	17, -13	
10	30	10	6.2	1.3	52	10, -9	
10	80	10	5.9	1.0	27	15, -10	Turned over
10	80	10	5.4	1.6	26	18, -10	
10	130	10	5.3	1.0	-12, 29	13, -10	
10	130	10	6.3	1.2	-7, 22	9, -10	
10	30	-10	5.6		-22		
10	30	-10	4.4		-15		
10	80	-10	2.8				
10	80	-10	5.2		-5		
10	130	-10	6.2		-5, 7		
10	30	-30	4.9		28, -17		
10	80	-30	5.3	1.4	41, -15	-9, 15	
10	80	-30	4.5	1.2	-8	-6, 11	
10	130	-30	3.2	1.3	22, -14	-13, 16	
10	130	-30	3.3	1.4	19, -19	11, 15	

TABLE IV.- MAXIMUM ACCELERATION DATA FOR HARD-SURFACE LANDINGS - Continued

(d) Configuration D

Vertical velocity, ft/sec	Horizontal velocity, ft/sec	Attitude, deg	Normal acceleration		Longitudinal acceleration		Angular acceleration		Remarks
			1st rock, g	2d rock, g	1st rock, g	2d rock, g	1st rock, radian/sec^2	2d rock, radians/sec^2	
5	30	33	6.5		3.8		19, -16		Turned over
5	80	33	6.2		4.1		19, -20		Turned over
5	30	30	5.1		3.2				Turned over
5	80	30	4.6		2.9				Turned over
5	30	20	3.4		2.7				Turned over
5	30	20	3.8		2.7				Turned over
5	30	20	3.2		2.5		17, -9		Turned over
5	80	20	4.8		2.5		14, -20		Turned over
5	80	20	3.2		2.0		17, -11		Turned over
5	80	20	4.4	2.3					
5	80	20	4.3	2.0	2.7	2.0	19, -14	-10, 11	
5	130	20	2.6	1.7	1.7	1.5	8, -14	-8, 12	Turned over
5	130	20	3.8	2.0	2.1	1.5	13, -11	-6, 11	
5	130	20	2.9	1.5	1.8	1.2	16, -9	-6, 10	Turned over
5	30	10	4.1	.8	1.7	.8	22, -5	-4, 4	
5	80	10	*	*	*	*	*	*	
5	130	10	*	*	*	*	*	*	
5	130	10	*	*	*	*	*	*	
5	30	-10	1.9		1.0		-10		
5	30	-10	3.0		1.2		-12		
5	80	-10	2.0	1.2	1.0	.9	-12		
5	80	-10	2.9	1.2	1.2	.9	-9		
5	130	-10	1.5	*	.9	*	-18	*	
5	130	-10	2.5	*	1.2	*	-12	*	
5	30	-30	2.3	1.2	1.4	.6	-16	4, -6	
5	80	-30	2.5	1.2	1.6	.7	-24, 7	9, -6	
5	80	-30	*	1.5	*	.4	*	6, -4	
5	130	-30	3.0	2.9	1.2	1.9	-36, 11	16, -9	
5	130	-30	2.8	2.8	1.1	1.9	-22, 11	12, -11	Turned over
5	130	-30	3.0	3.3	1.0	1.1	-22, 11	10, -14	Turned over

*No acceleration data obtained because of model bouncing during rocking motion.

TABLE IV.- MAXIMUM ACCELERATION DATA FOR HARD-SURFACE LANDINGS - Concluded

(e) Configuration D - Concluded

Vertical velocity, ft/sec	Horizontal velocity, ft/sec	Attitude, deg	Normal acceleration		Longitudinal acceleration		Angular acceleration		Remarks
			1st rock, g	2d rock, g	1st rock, g	2d rock, g	1st rock, radians/sec^2	2d rock, radians/sec^2	
10	30	33	*		*		*		Turned over
10	30	33	*		*		*		Turned over
10	30	33	*		*		*		Turned over
10	30	33	*		*		*		Turned over
10	80	33	*		*		*		Turned over
10	80	33	12.2		-3.7, 3.3		55, -12		Turned over
10	80	33	*		*		*		Turned over
10	80	33	*		*		*		Turned over
10	30	20	8.5		3.8		17, -16		Turned over
10	30	20	8.1		3.1				Turned over
10	80	20	6.9		3.0				Turned over
10	80	20	5.1		3.3				Turned over
10	80	20	6.2		3.4		9, -19		Turned over
10	130	20	5.0		2.1				Turned over
10	30	10	*	1.9	*	1.2	*	-4, 8	
10	30	10	*	1.8	*	1.4	*	-6, 6	
10	80	10	*	1.1	*	1.1	*	-4, 7	
10	80	10	*	2.2	*	1.1	*	-6, 8	
10	130	10	7.9	1.9	1.0	1.0	-18	-7, 9	
10	130	10	8.3	1.5	1.1	1.1	-14	-7, 6	
10	30	-10	*	*	*	*	*	*	
10	30	-10	*	*	*	*	*	*	
10	80	-10	*	*	*	*	*	*	
10	80	-10	*	*	*	*	*	*	
10	130	-10	*	1.8	*	1.0	*	9, -12	
10	130	-10	*	*	*	.8		7, -9	
10	30	-30	*	*	*	*	*	*	
10	30	-30	*	*	*	*	*	*	
10	80	-30	*	1.2	*	.4		8, -4	
10	80	-30	*	1.5	*	.5	*	7	
10	130	-30	6.1	*	1.0	*	-14.5	*	Turned over
10	130	-30	*	1.6	*	.9	*	9, -8	

*No acceleration data obtained because of model bouncing during rocking motion.

TABLE V.- MAXIMUM ACCELERATION DATA FOR LANDINGS ON WATER

[Configuration C]

Vertical velocity, ft/sec	Horizontal velocity, ft/sec	Attitude, deg	Normal acceleration			Longitudinal acceleration			Angular acceleration			Remarks
			1st impact, g	2d impact, g	3d impact, g	1st impact, g	2d impact, g	3d impact, g	1st impact, radians/sec^2	2d impact, radians/sec^2	3d impact, radians/sec^2	
5	50	20	1.6	1.4	0.5	0.7	-0.1, 1.0	0.6	-7, 11	-7, 16	10	
5	50	20	1.7	1.5	.4	.8	1.1	.6	-7, 9	-9, 14	5	
5	80	20	1.4	2.3	2.1	.5	-.1, 1.0	-.5, 1.4	-8, 7	-11, 14	-19, 21	
5	80	20	1.7	2.8	1.8	.6	-.3, 1.3	-.4, 1.6	-6, 8	-15, 20	-19, 23	
5	80	20	1.7	2.8	1.8	.5	-.2, 1.4	-.5, 1.6	-7, 7	-14, 19	-20, 23	
5	130	20	1.6	8.9		.3, -.8	3.0, -.8		-12, 3	48, -25		Turned over
5	130	20	.8	1.8	7.9	.3	.5, -.7	3.0, -.6	-14, 4	-7, 8	42, -19	Turned over
5	130	20	1.4	2.7	9.5	.3	.7, -1.3	4.4	-12	-11	74, -30	Turned over
5	50	0	2.4	1.3		1.1, -.5	-1.2, 1.4		21, -11	-26, 28		
5	50	0	2.8	1.3		1.1, -.5	-1.2, 1.4		23, -10	-26, 28		
5	80	0	4.8	5.1		1.7, -1.0	-1.2, 1.5		30, -19	-57, 34		
5	130	0	10.4			3.0, -1.7			52, -33			Turned over
5	130	0	10.6			2.4, -1.8			46, -32			Turned over

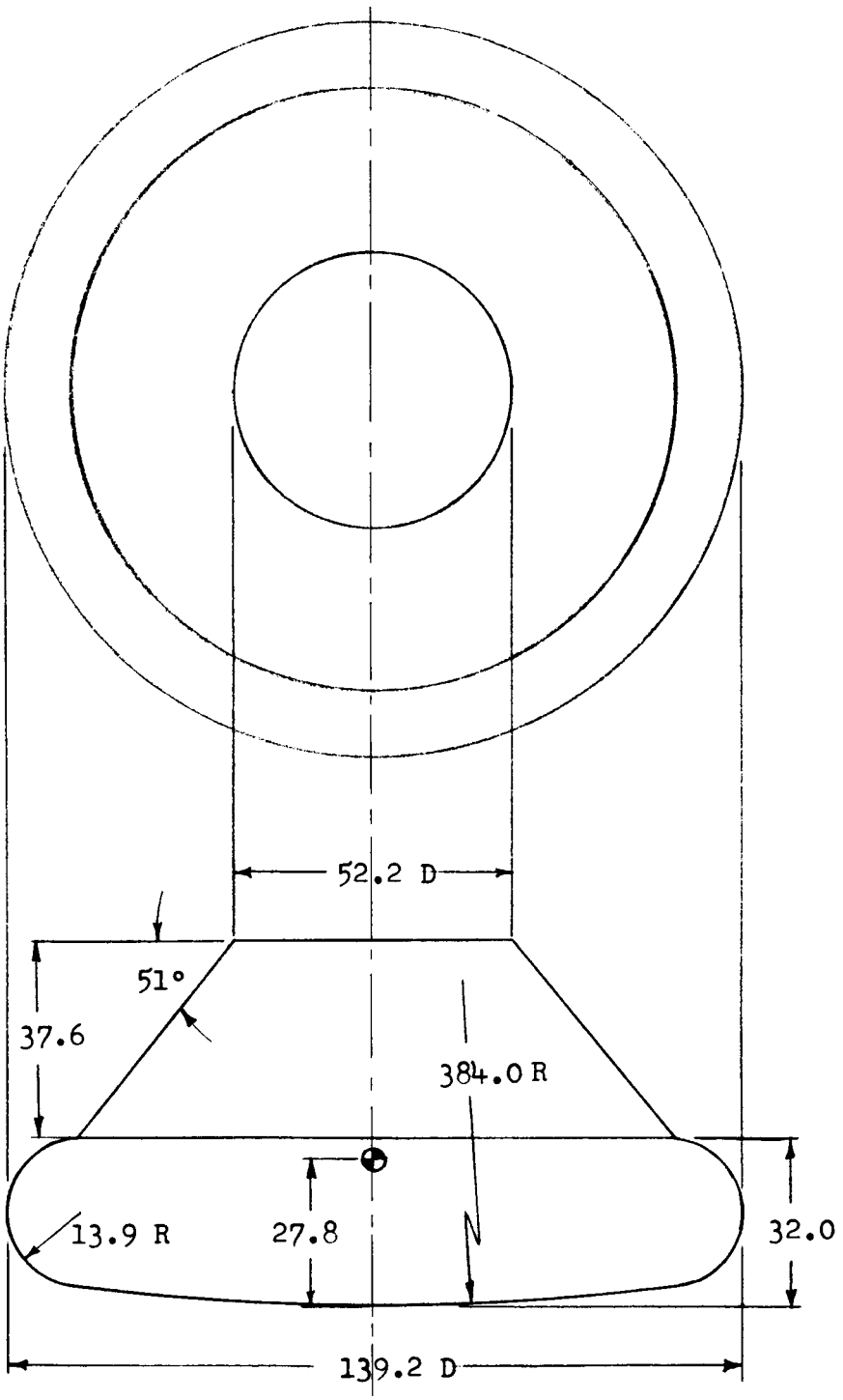

(a) Configuration A.

Figure 1.- General arrangement of 1/8-scale dynamic model of a reentry capsule. (All dimensions are in inches full scale.)

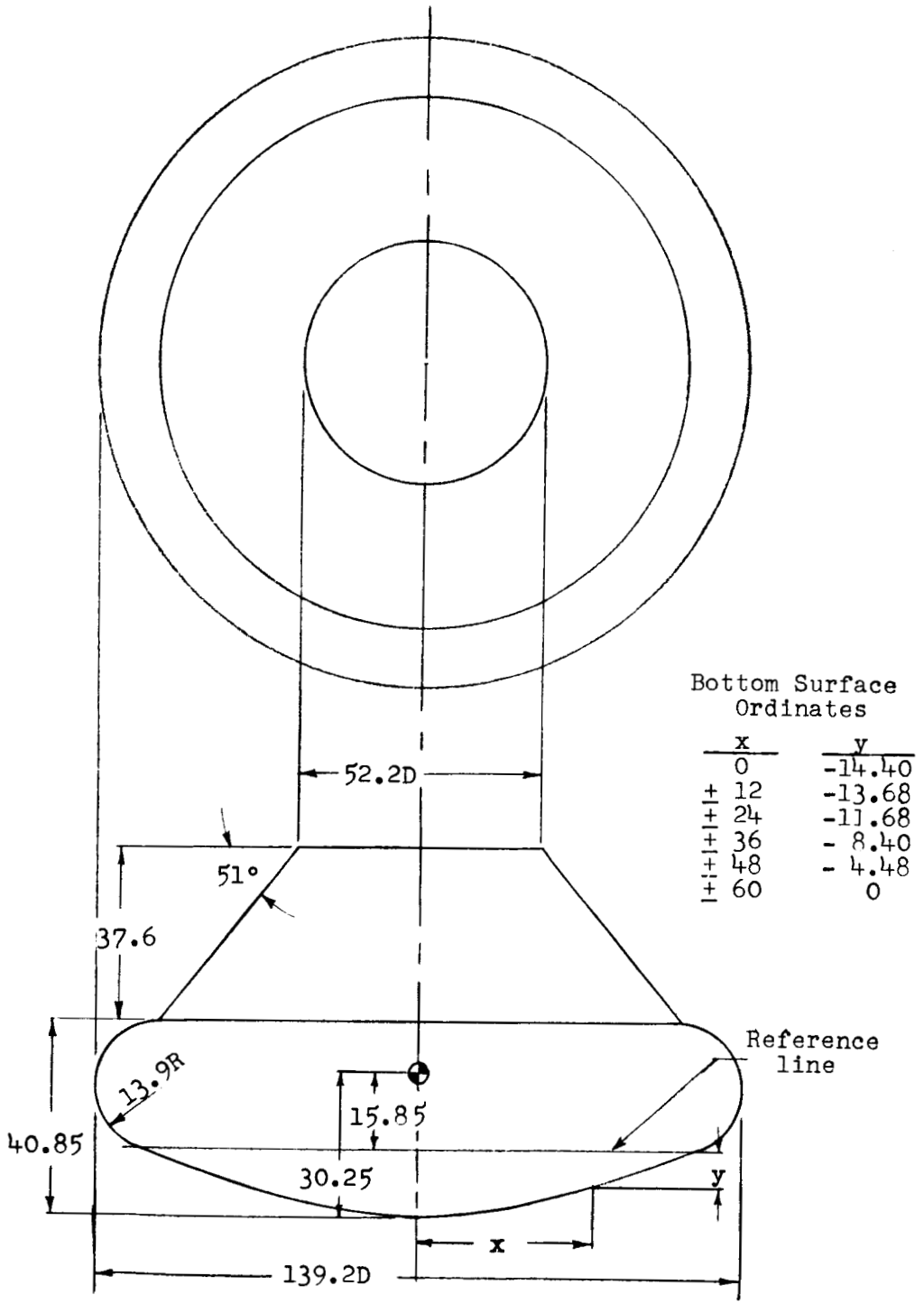

(b) Configuration B.

Figure 1.- Continued.

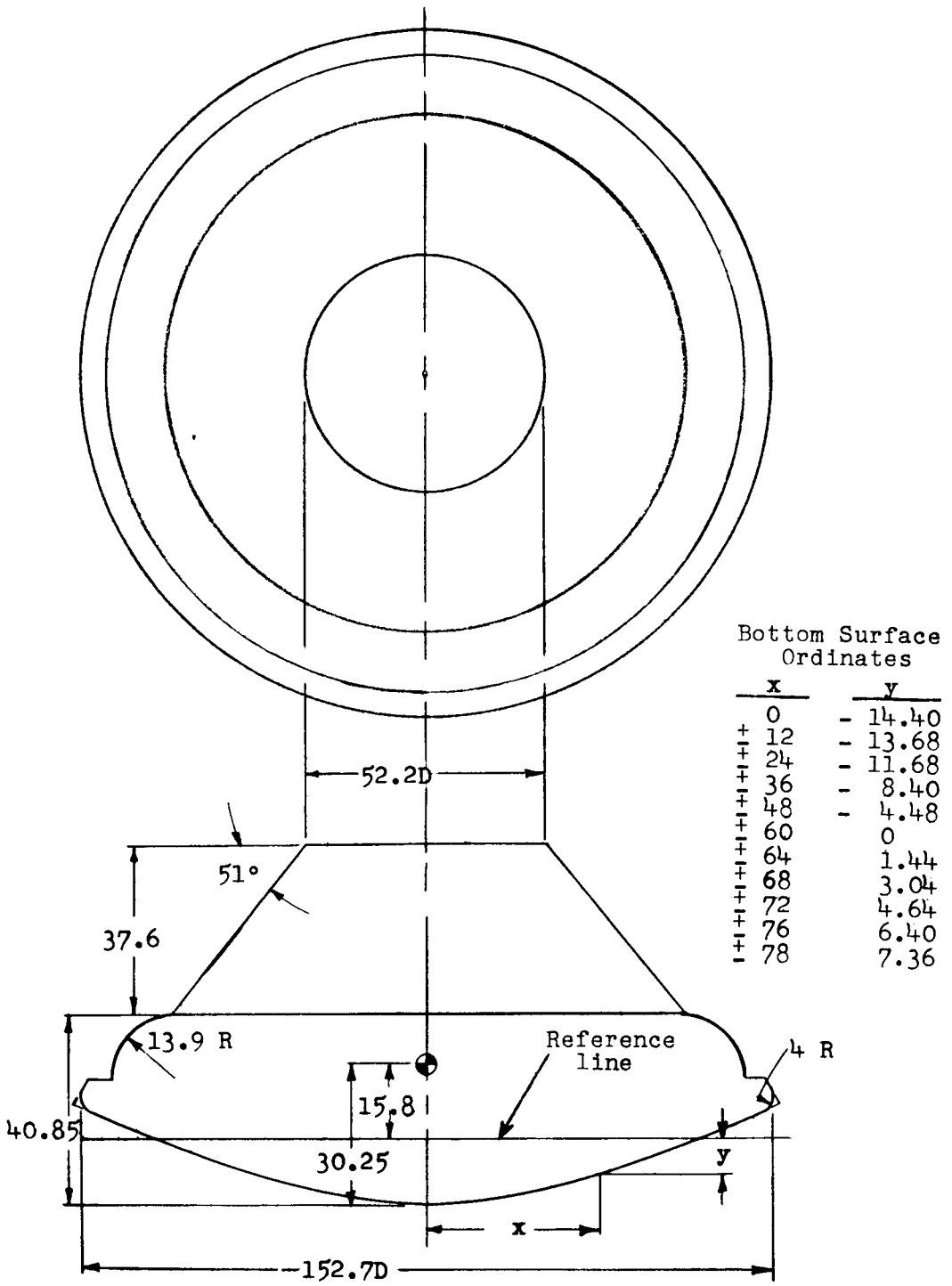

Bottom Surface Ordinates

x	y
0	- 14.40
± 12	- 13.68
± 24	- 11.68
± 36	- 8.40
± 48	- 4.48
± 60	0
± 64	1.44
± 68	3.04
± 72	4.64
± 76	6.40
± 78	7.36

(c) Configuration C.

Figure 1.- Concluded.

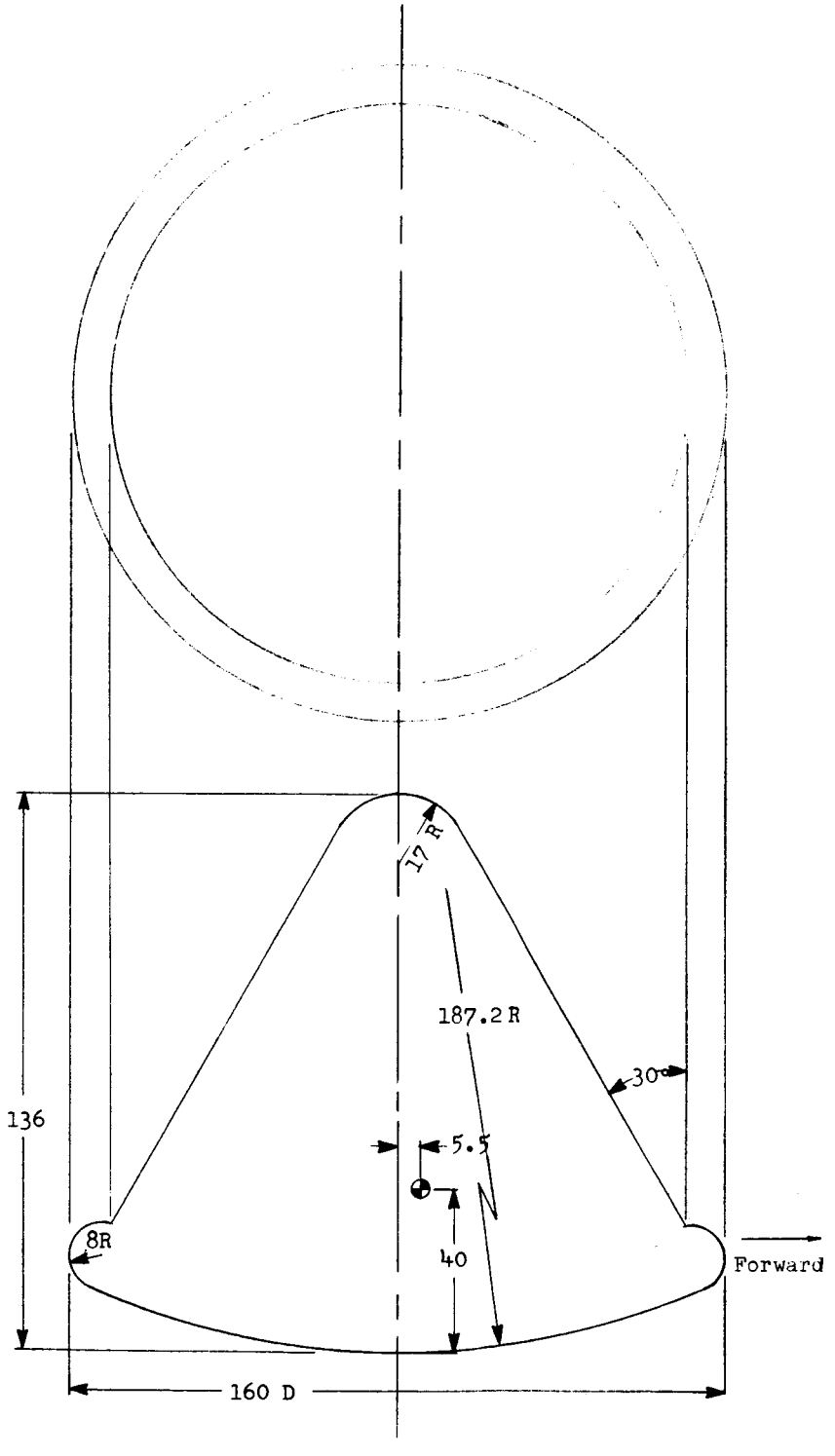

Figure 2.- General arrangement of 1/10-scale dynamic model of a reentry capsule. Configuration D. (All dimensions are in inches full scale.)

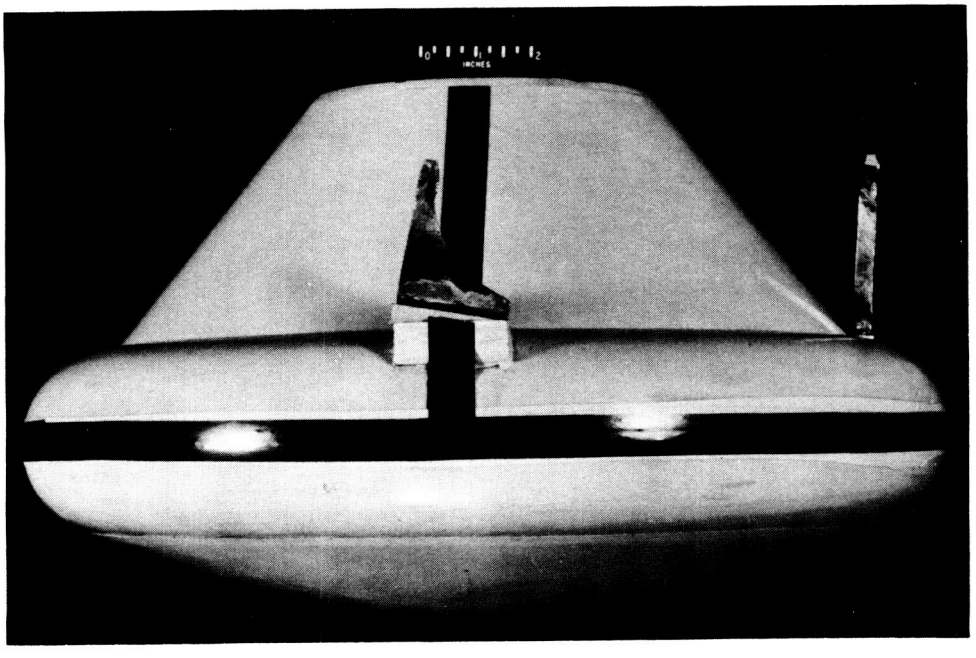

L-61-2900

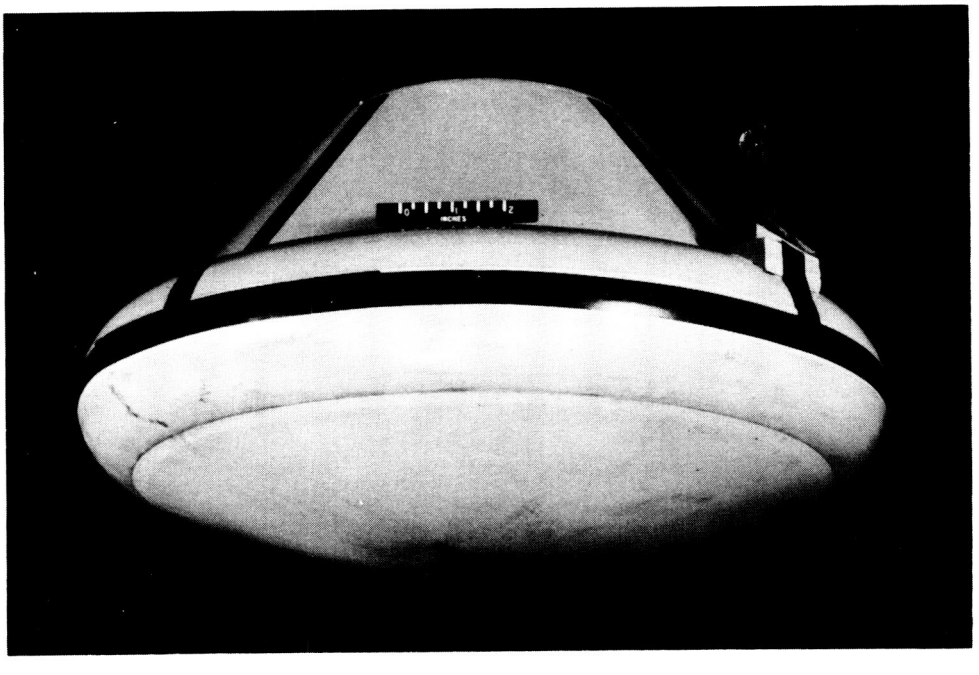

L-61-2901

Figure 3.- Photographs of configuration B.

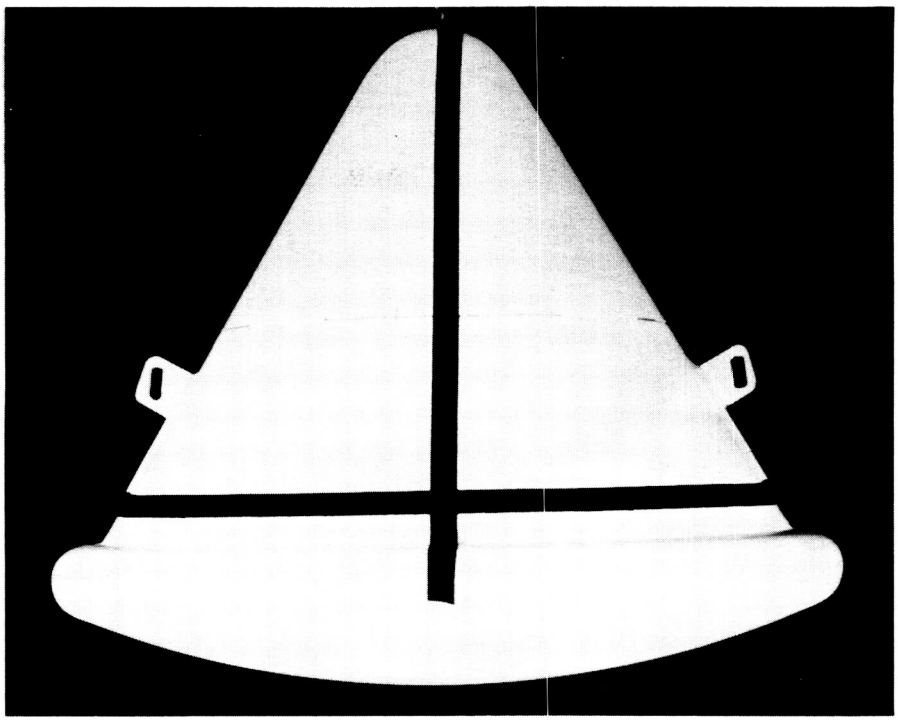

L-61-6619

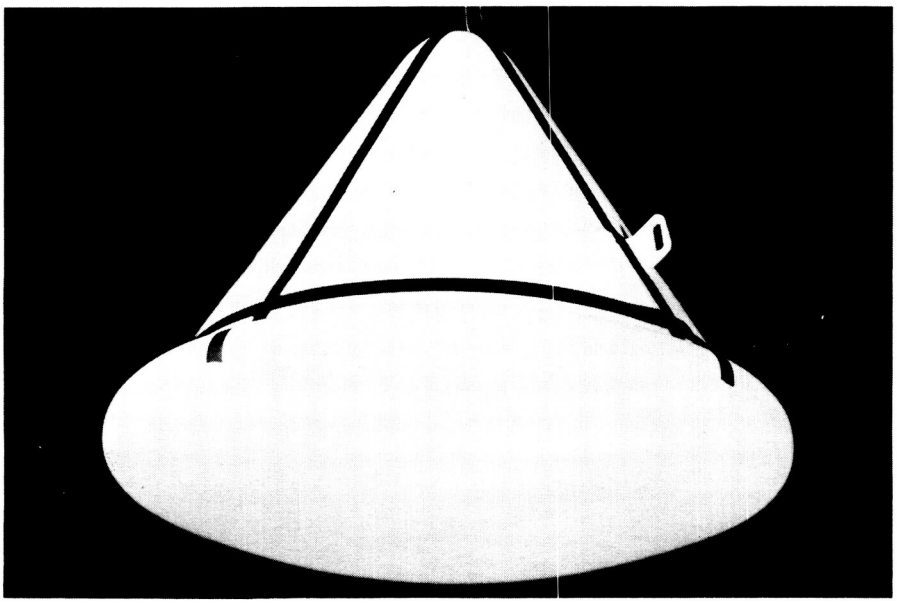

L-61-6618

Figure 4.- Photographs of configuration D.

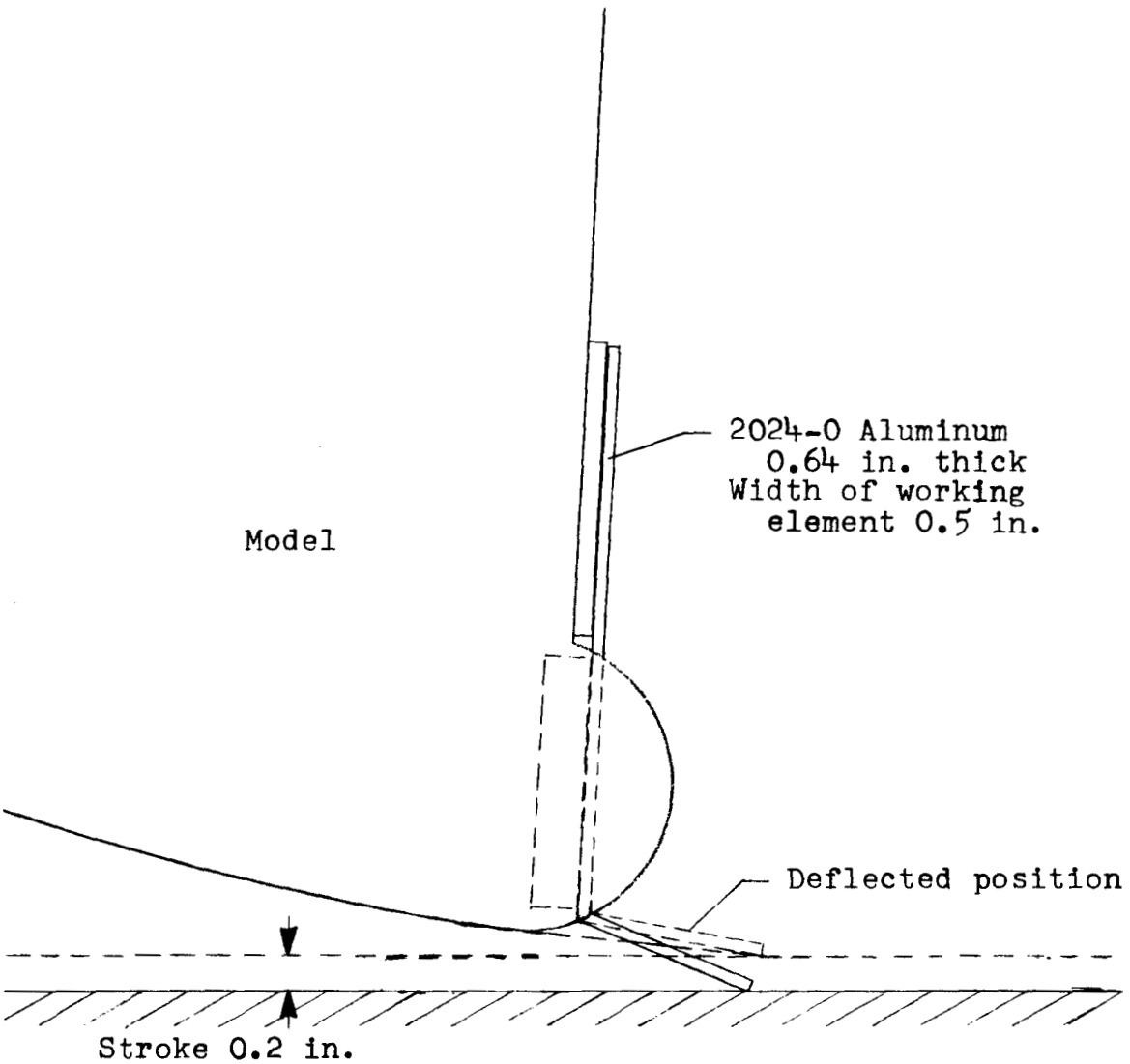

Figure 5.- Sketch showing yielding metal shock absorber on configuration D. (All dimensions are model size.)

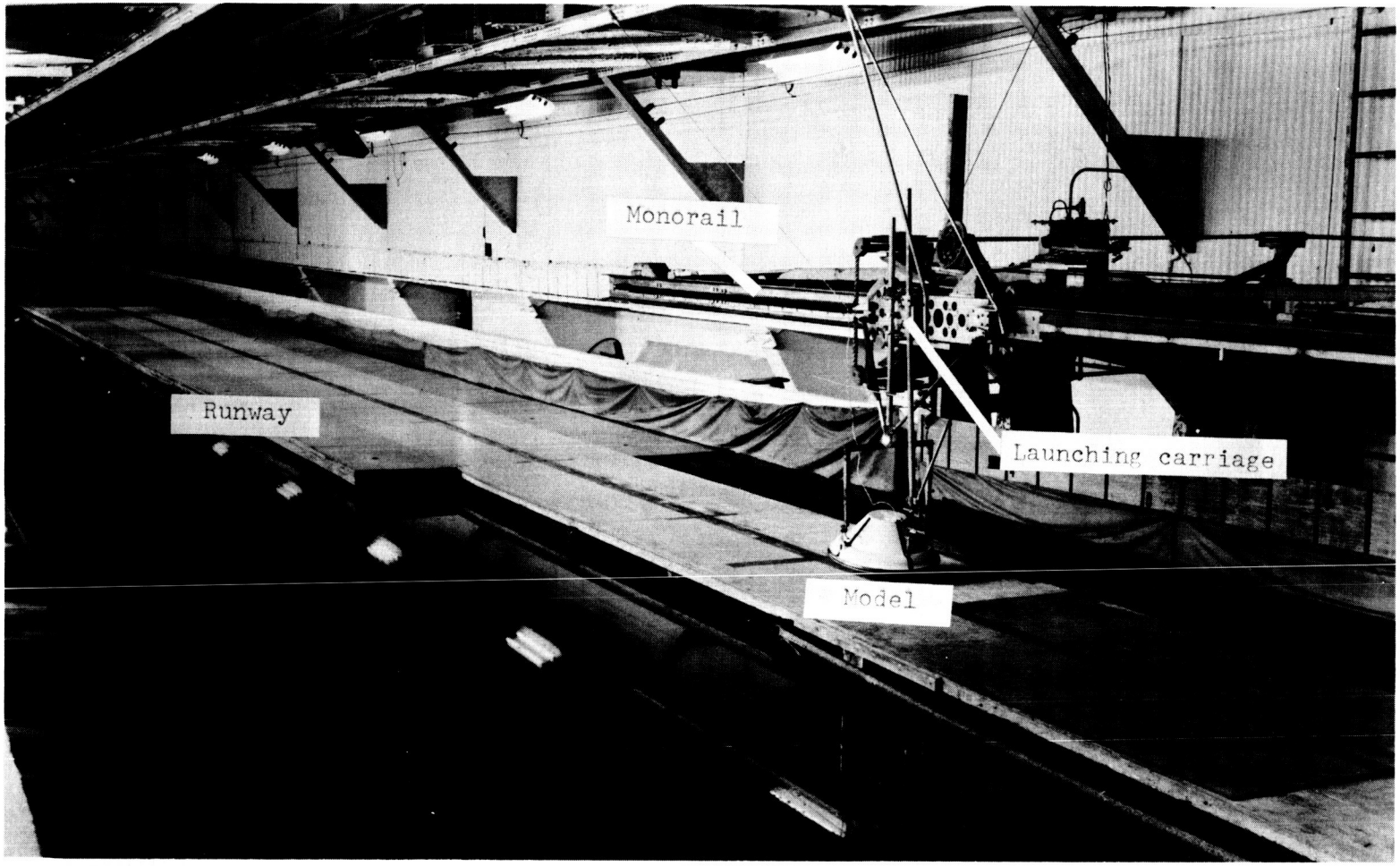

(a) Hard-surface runway. L-61-3178.1

Figure 6.- Photographs of test apparatus.

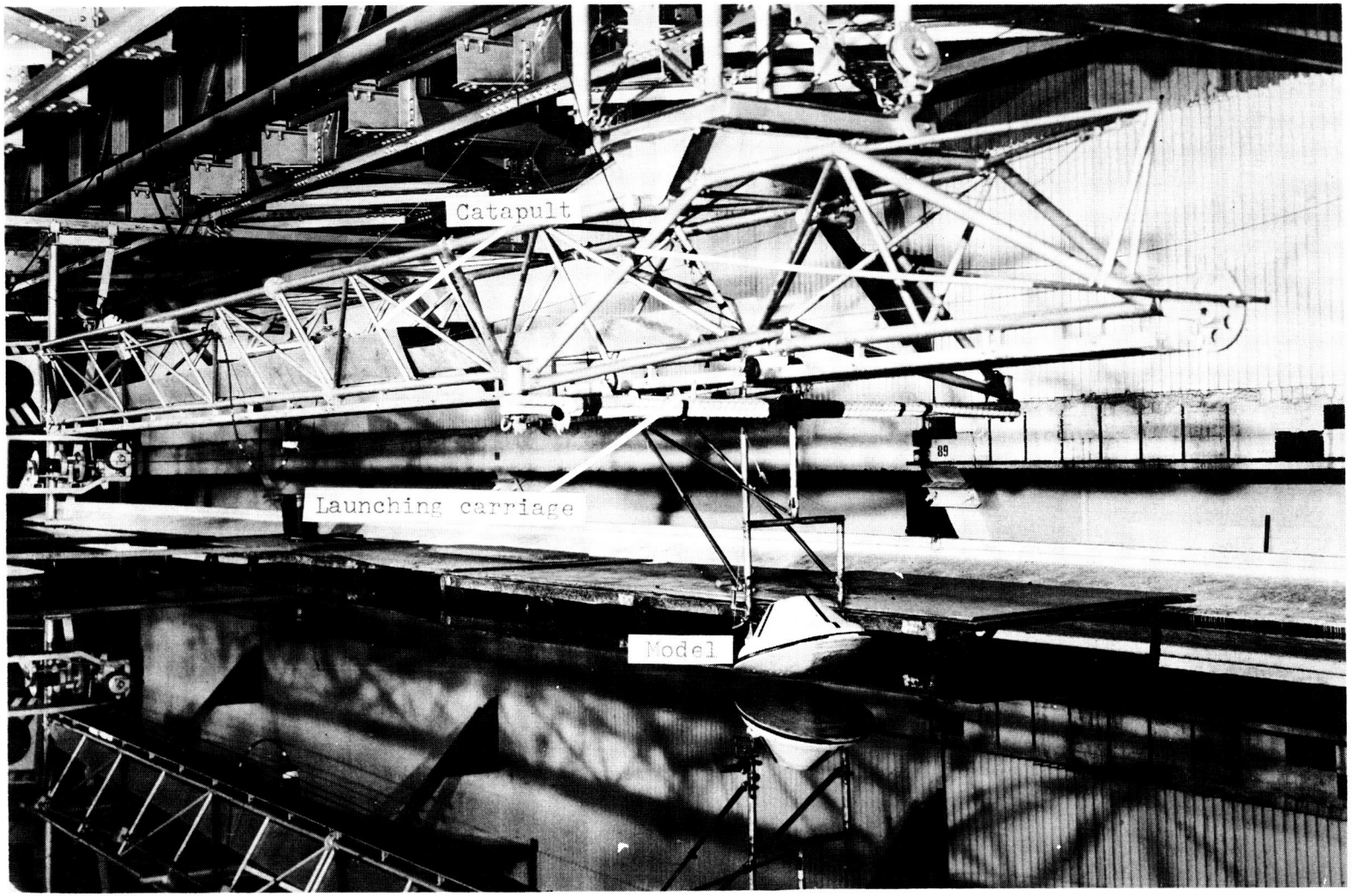

(b) Water-landing area.

L-61-6615.1

Figure 6.- Concluded.

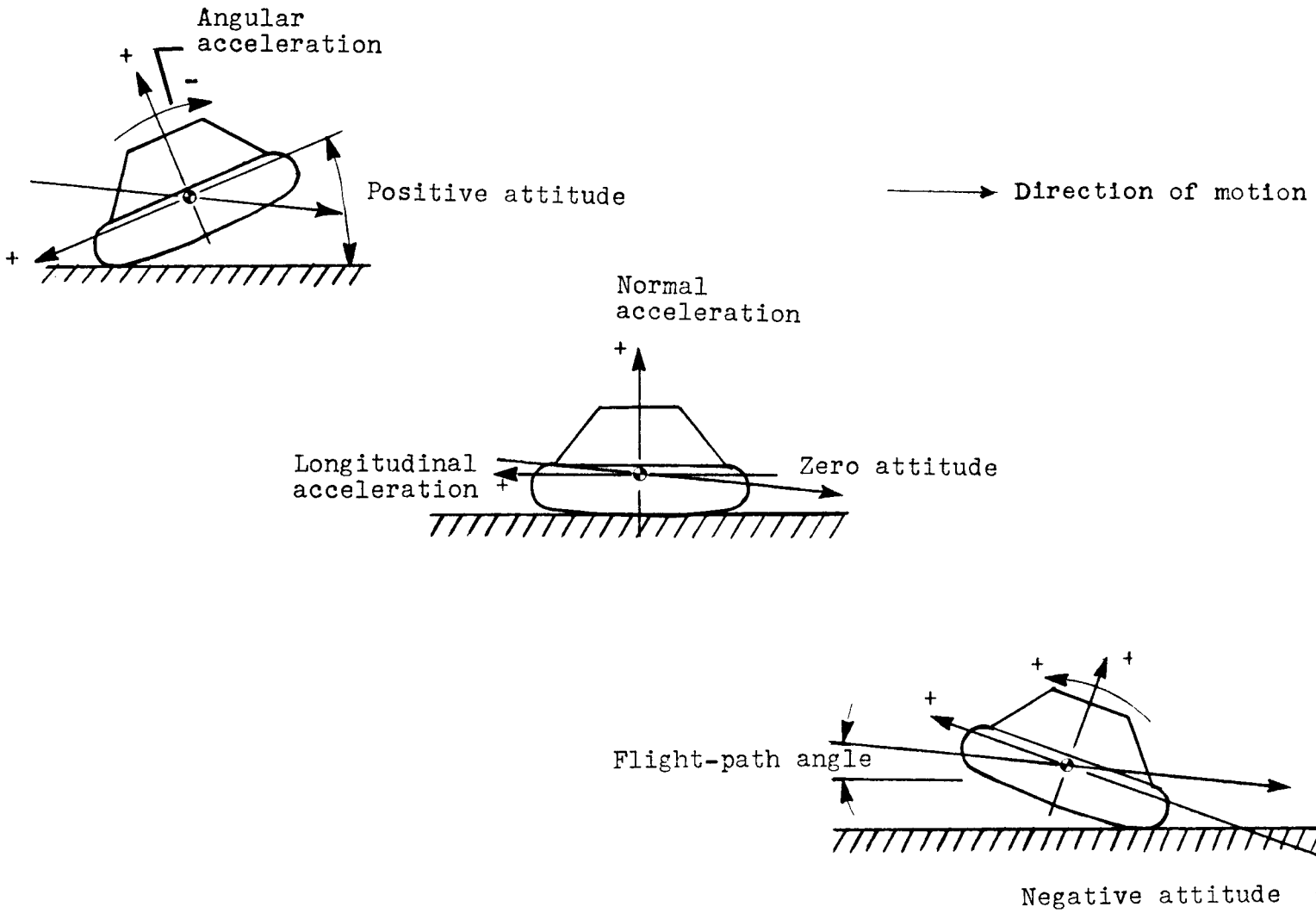

Figure 7.- Sketches identifying acceleration axes, attitudes, force directions, and flight path.

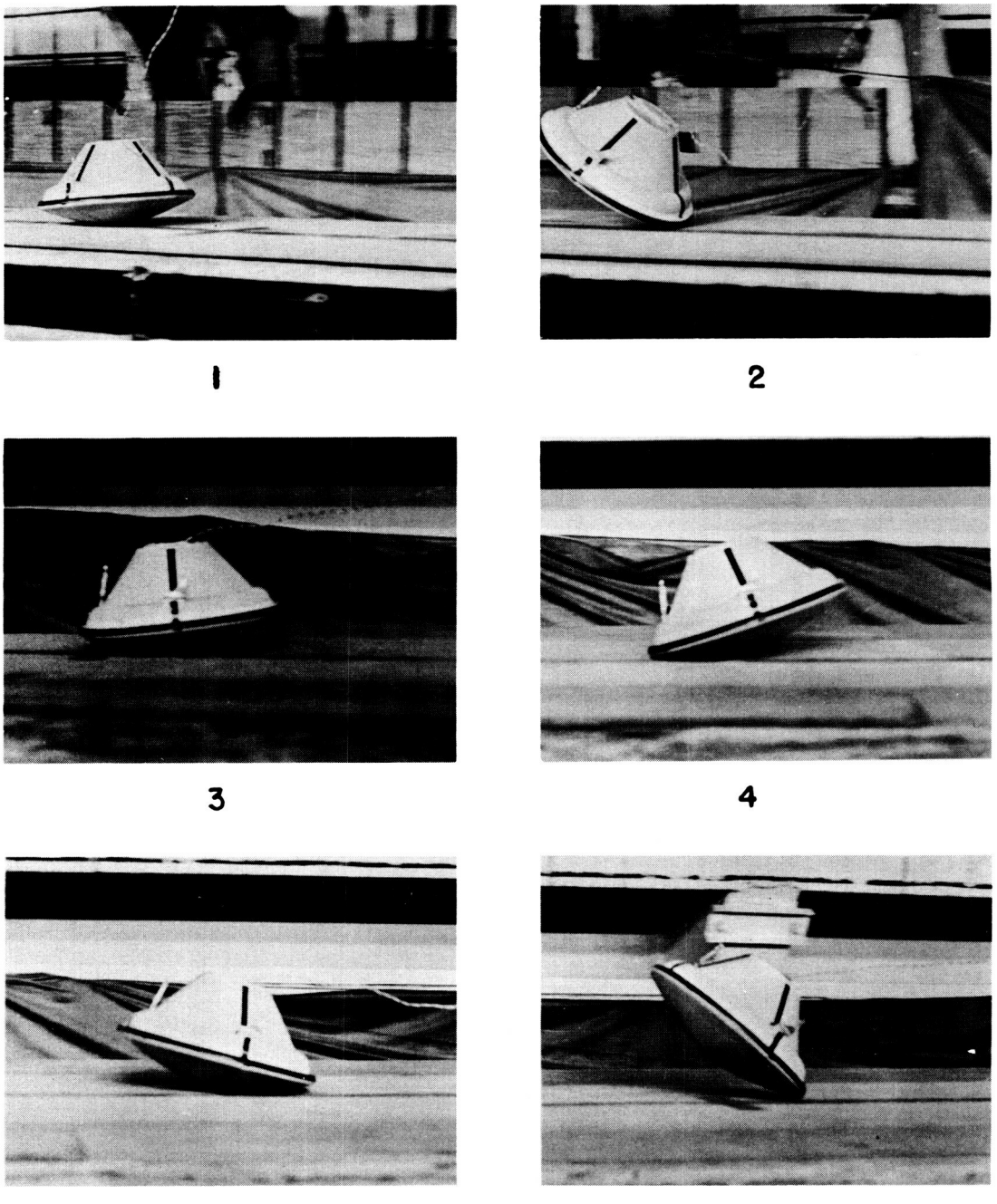

(a) Vertical velocity, 10 ft/sec; landing attitude, 10°. L-61-4811

Figure 8 .- Sequence photographs during typical landings of configuration C on hard-surface runway. Horizontal velocity, 80 ft/sec.

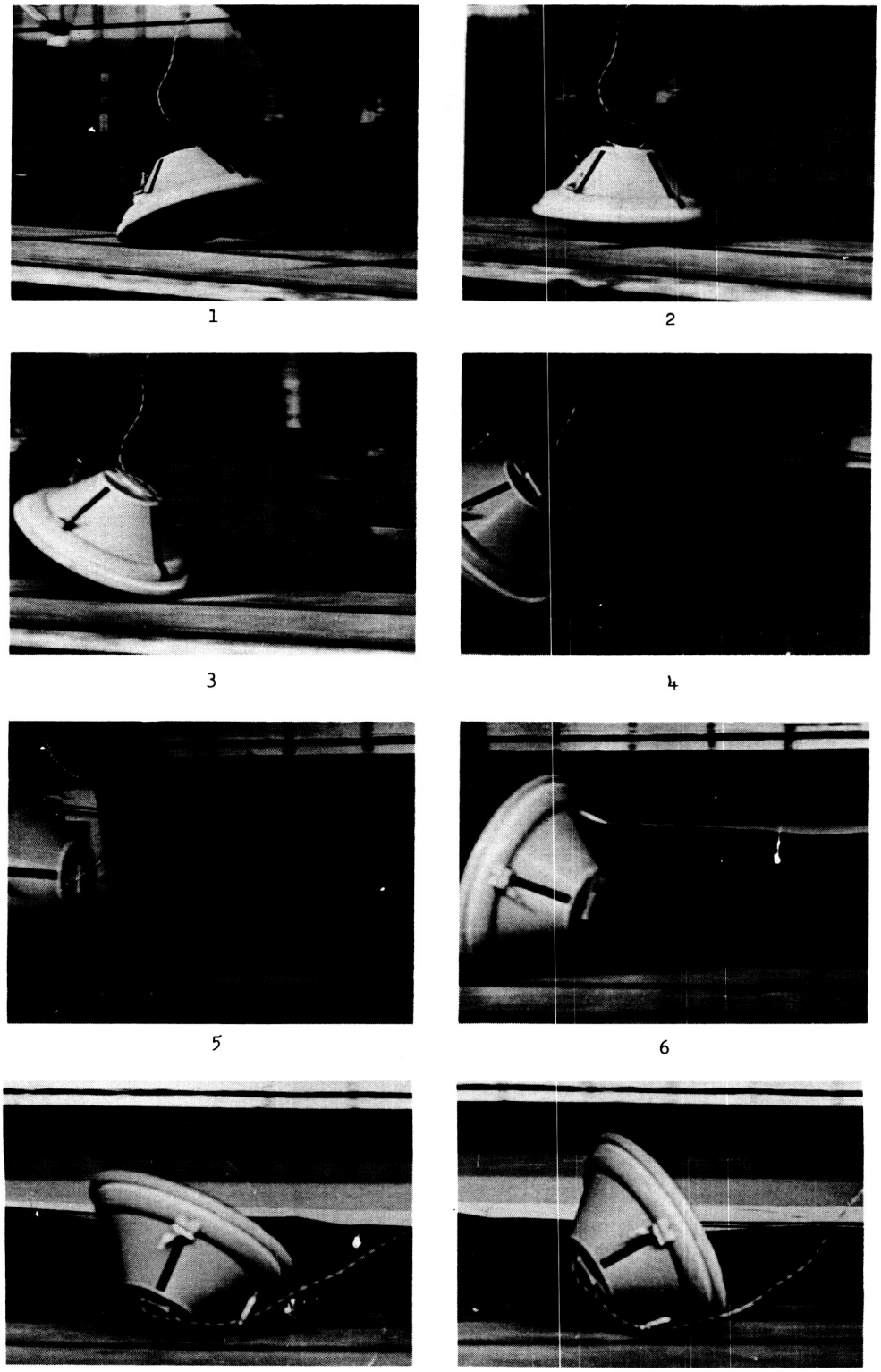

(b) Vertical velocity, 5 ft/sec; landing attitude, 30°. L-63-14

Figure 8.- Concluded.

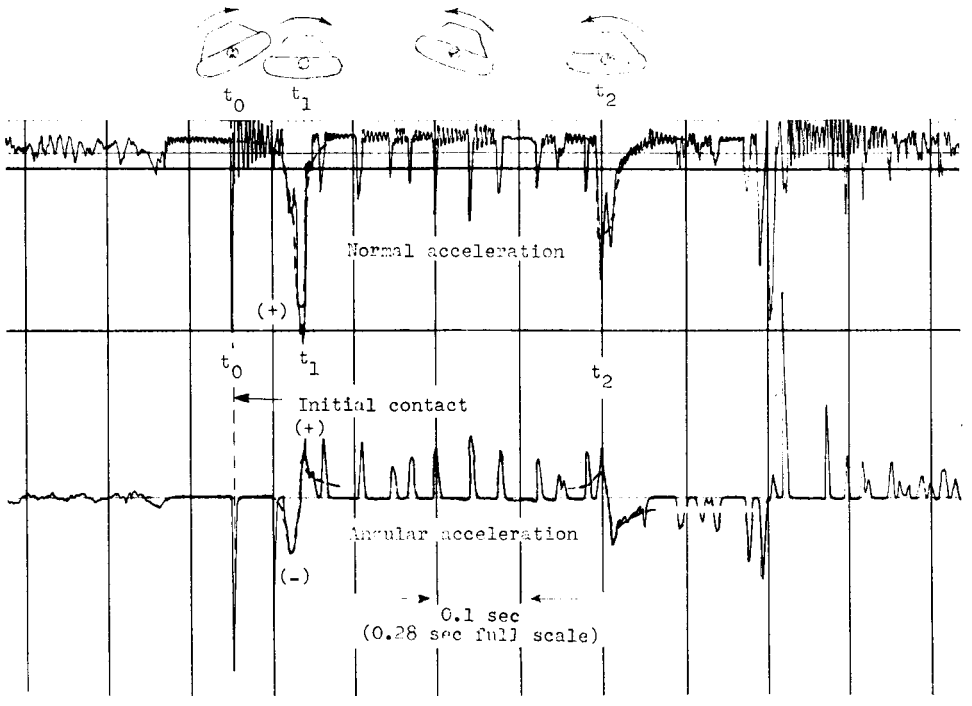

(a) Configuration A.

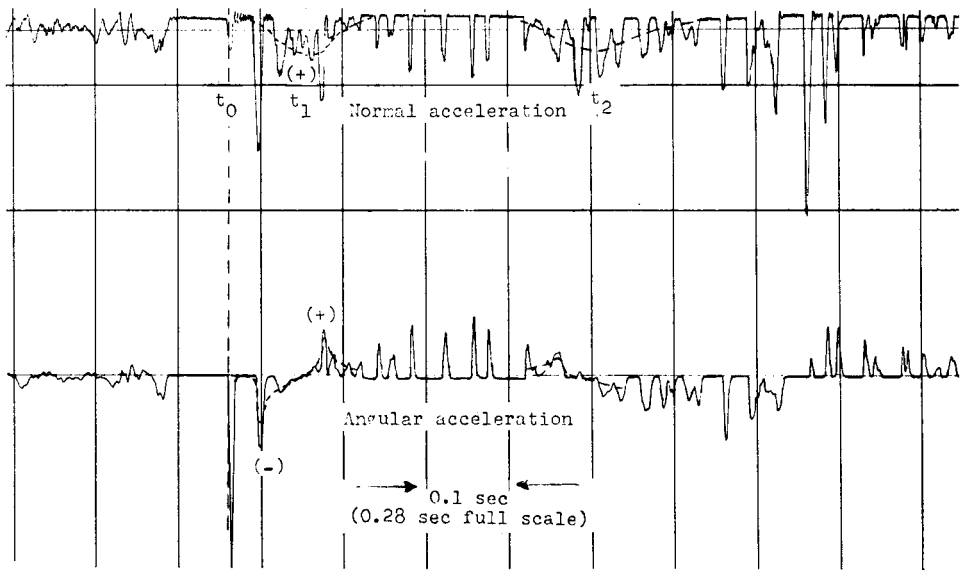

(b) Configuration B.

Figure 9.- Typical acceleration time histories of the four configurations tested. Vertical velocity, 5 ft/sec; horizontal velocity, 130 ft/sec; landing attitude, 20°; hard-surface landing.

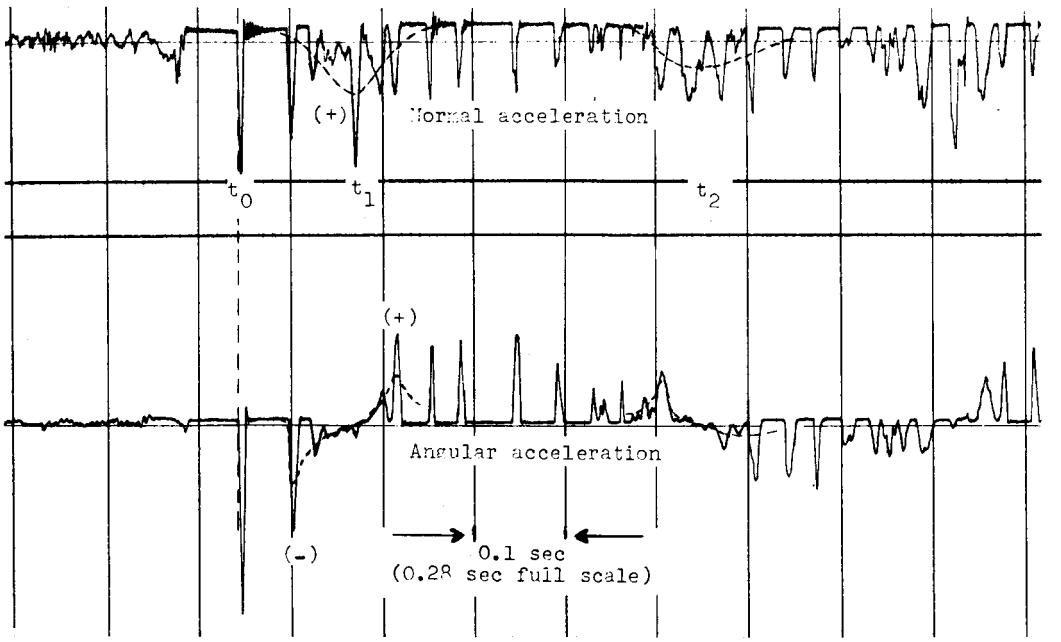

(c) Configuration C.

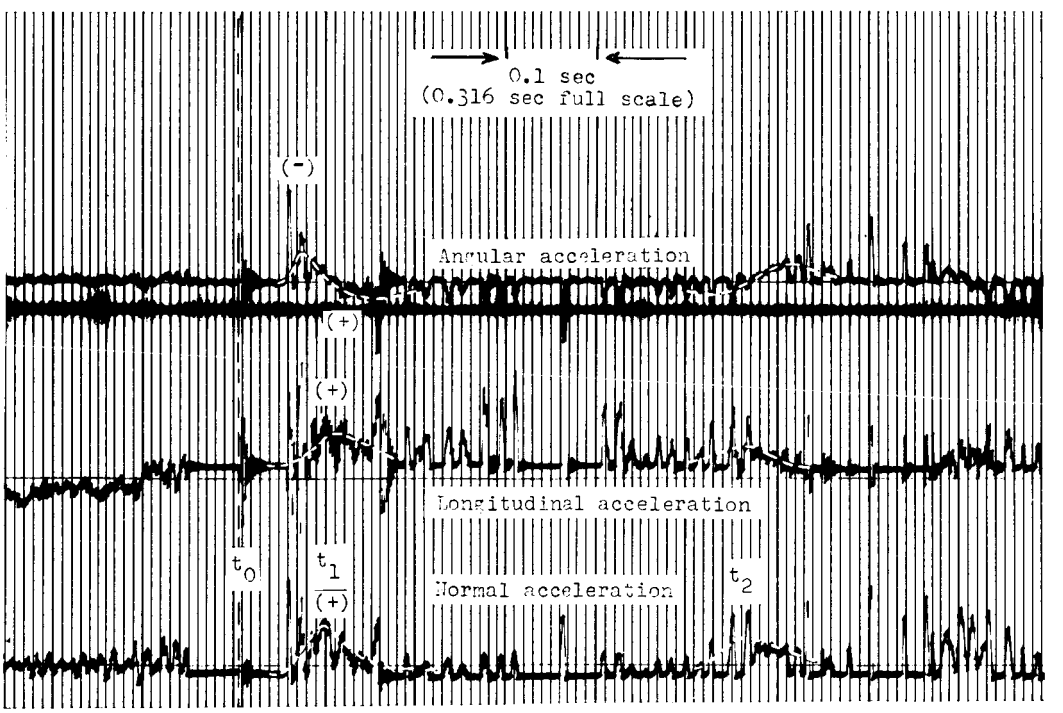

(d) Configuration D.

Figure 9.- Concluded.

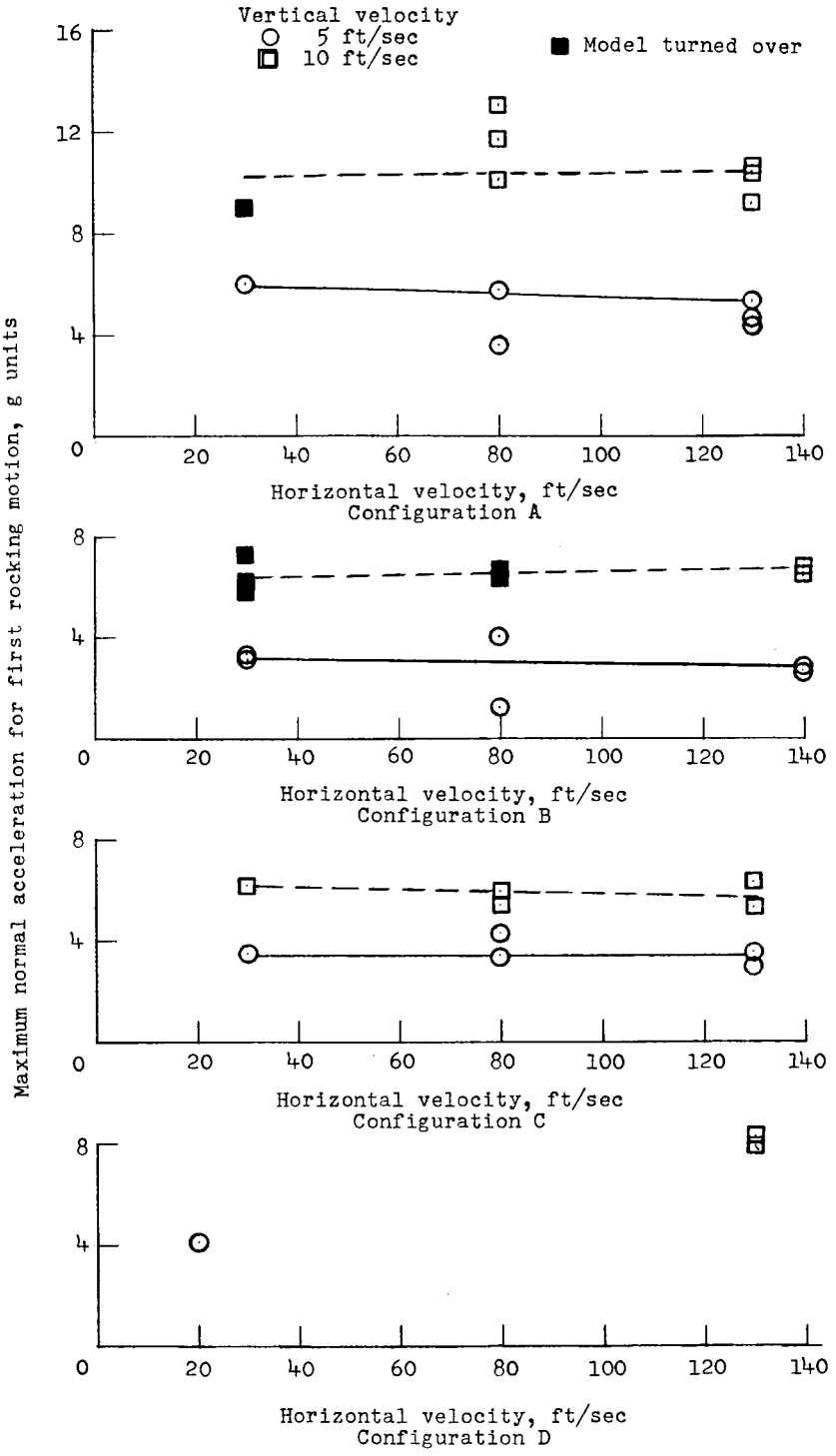

Figure 10.- Normal landing acceleration comparison for configurations A, B, C, and D for vertical velocities of 5 and 10 ft/sec over a range of horizontal velocities. Landing attitude 10°; hard-surface landings.

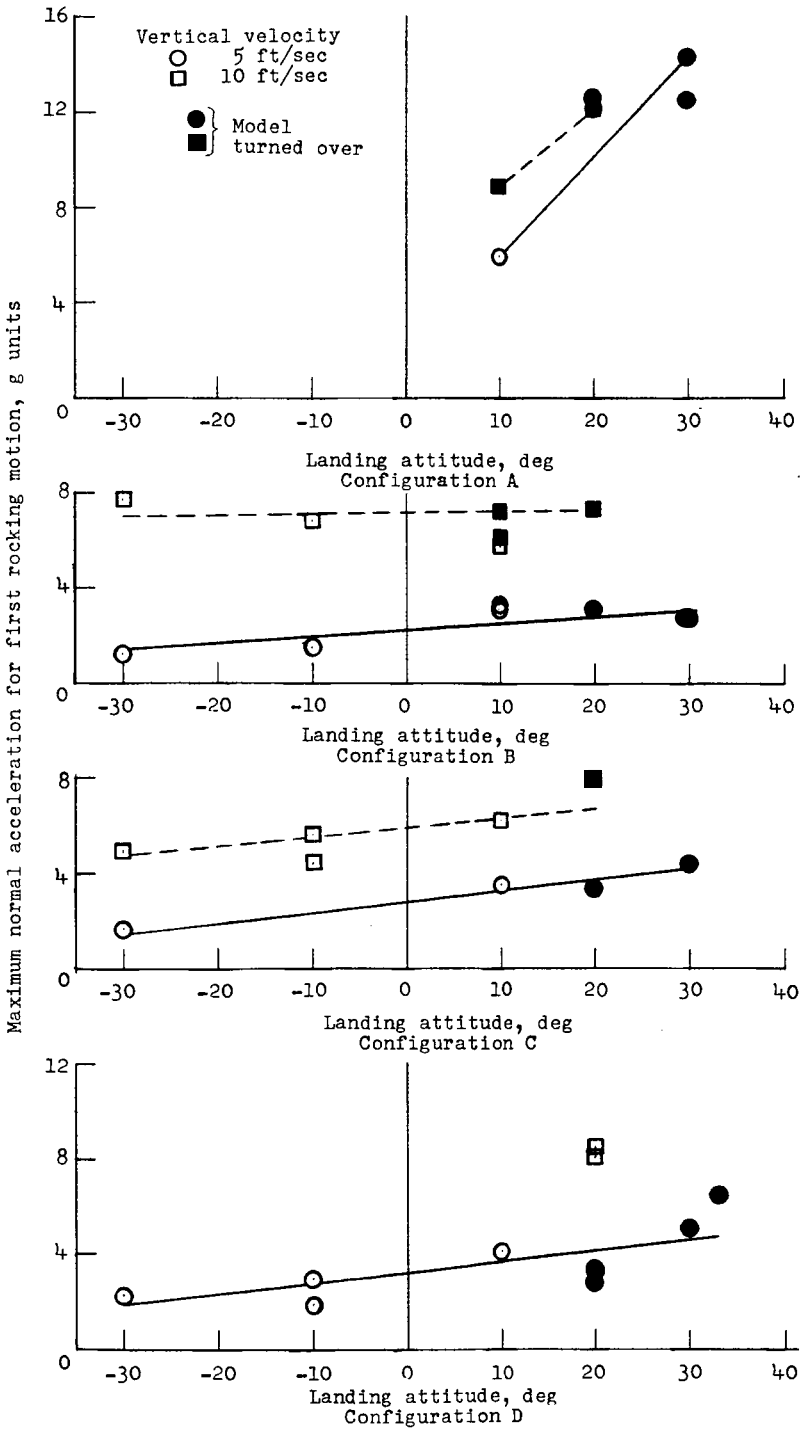

(a) Horizontal velocity, 30 ft/sec.

Figure 11.- Normal landing acceleration comparison for landing attitudes tested. Hard-surface landings.

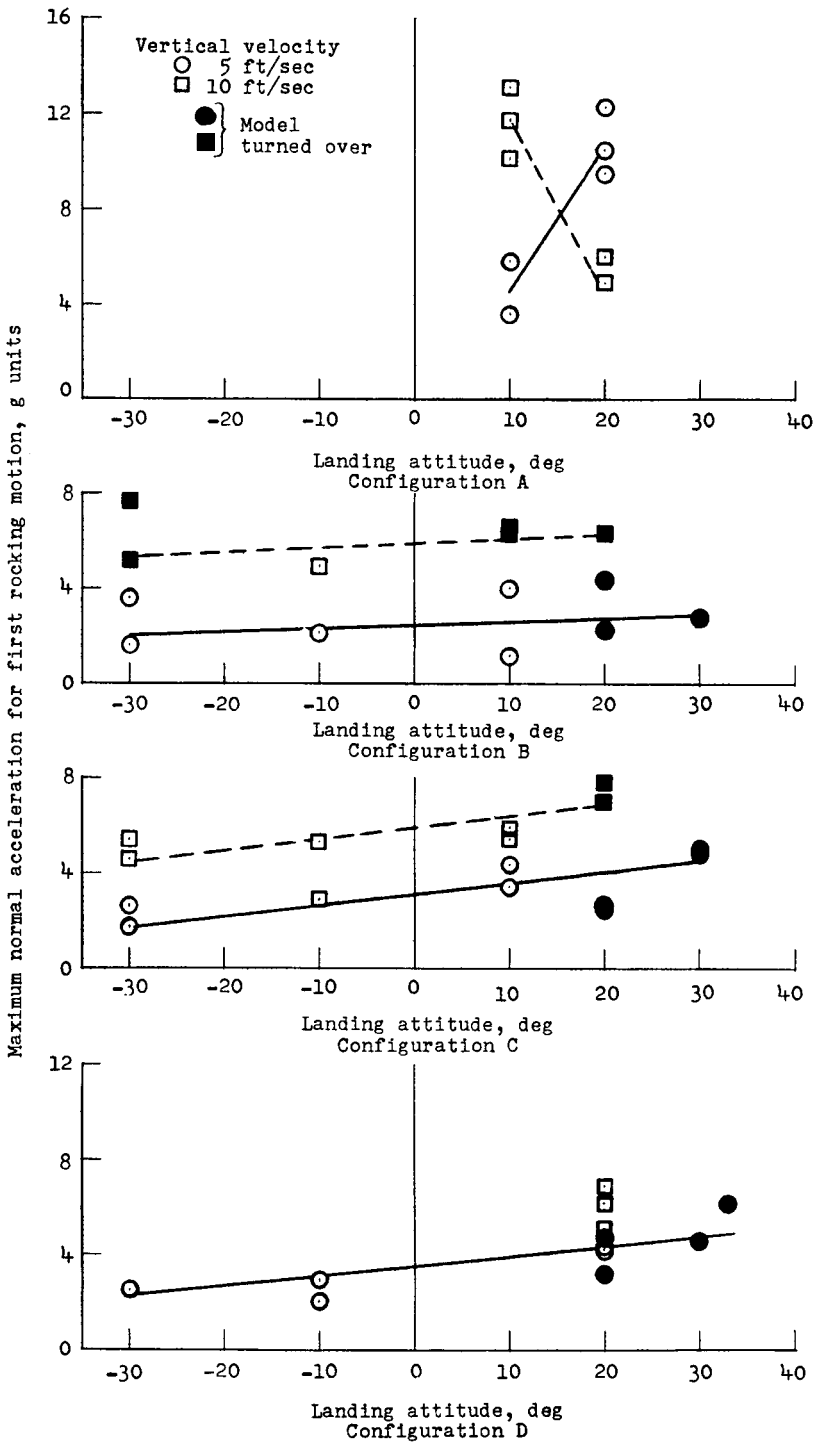

(b) Horizontal velocity, 80 ft/sec.

Figure 11.- Continued.

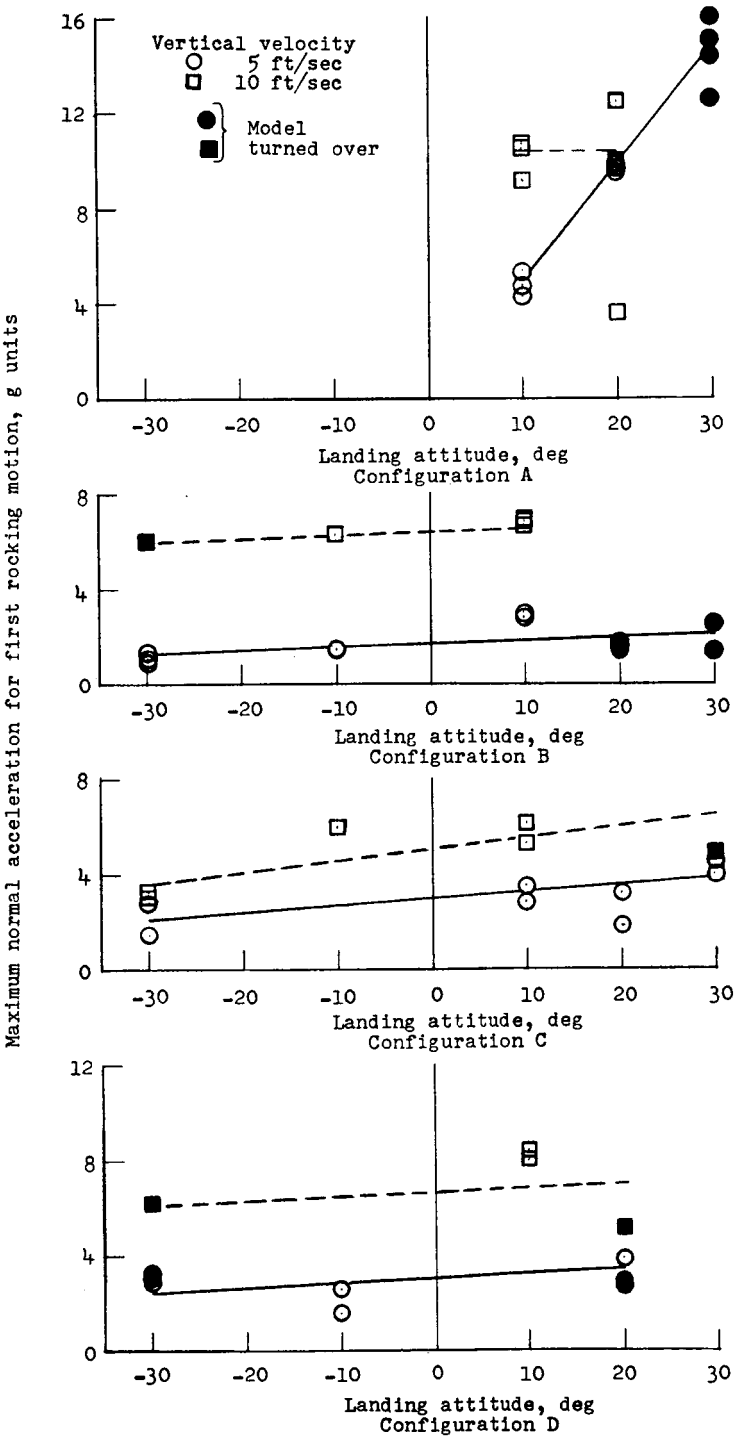

(c) Horizontal velocity, 130 ft/sec.

Figure 11.- Concluded.

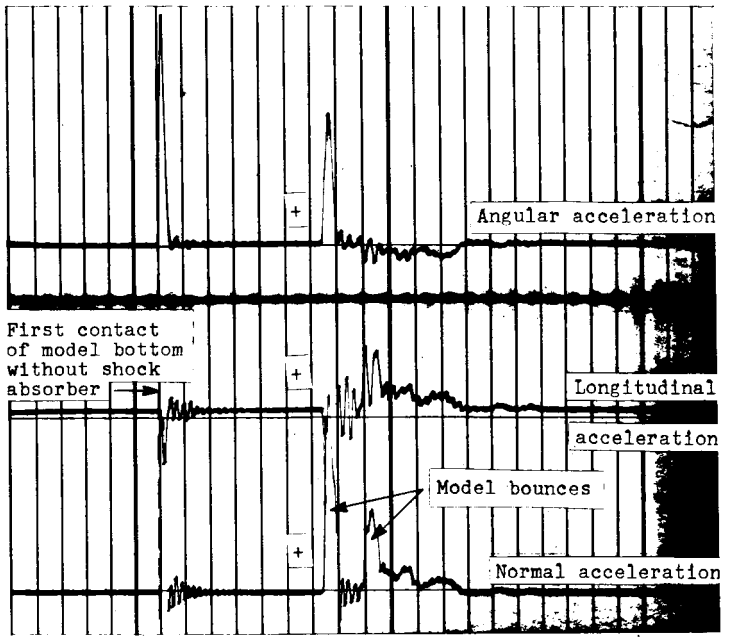

(a) Without shock absorber.

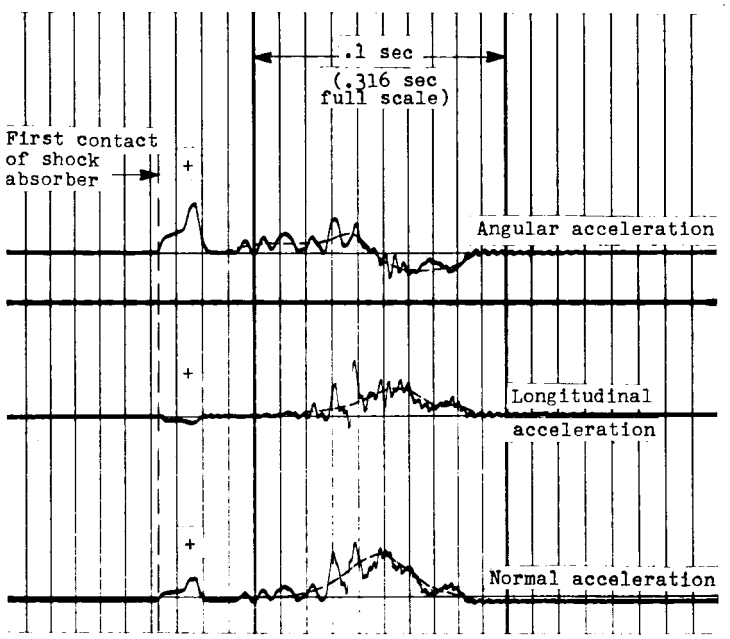

(b) With shock absorber.

Figure 12.- Typical oscillograph records of accelerations of configuration D without and with a shock absorber. Vertical velocity, 10 ft/sec; horizontal velocity, 80 ft/sec; landing attitude, 33°; hard-surface landings.

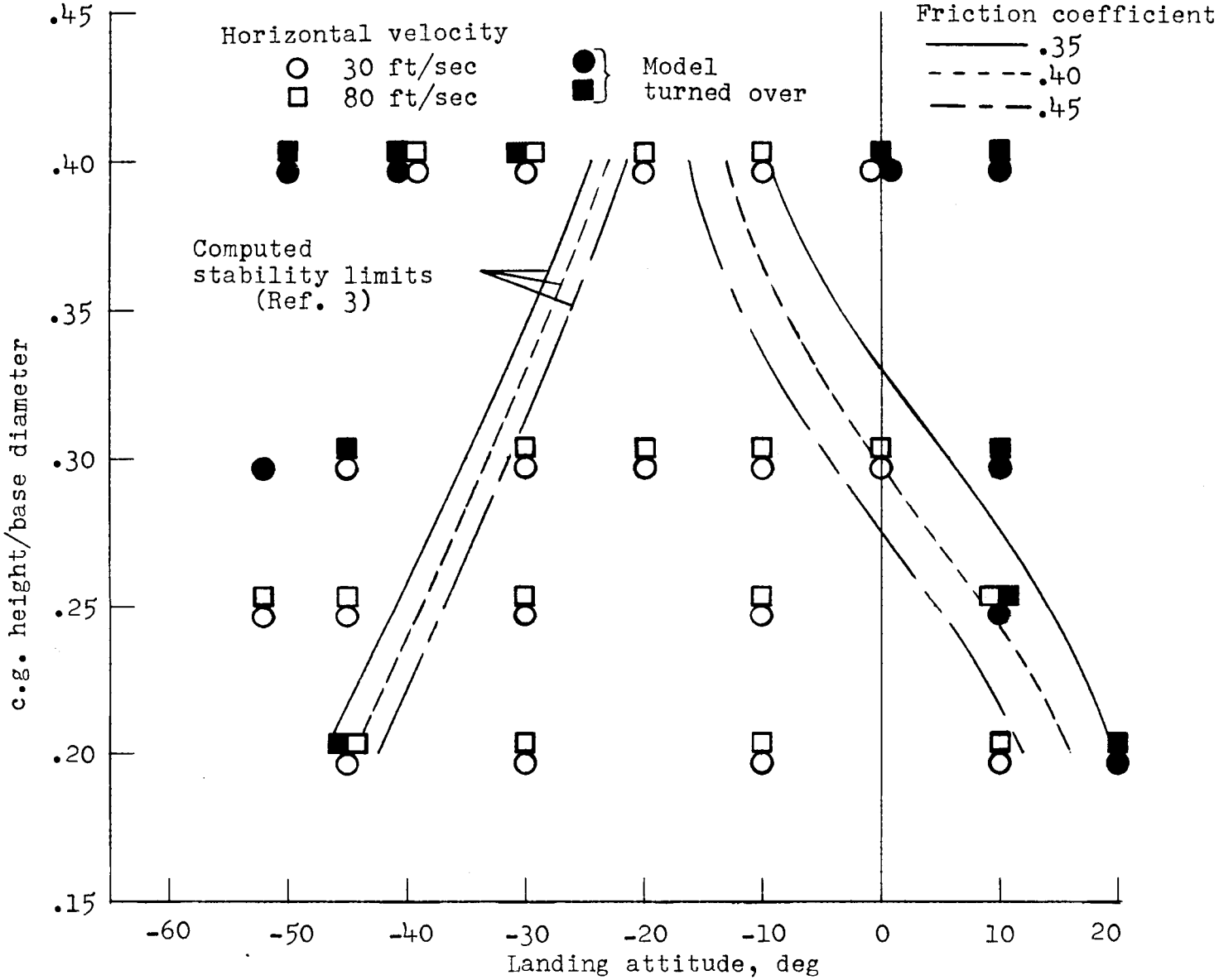

Figure 13.- Stability limits for configuration C with various center-of-gravity locations. Vertical velocity, 10 ft/sec; hard-surface landings.

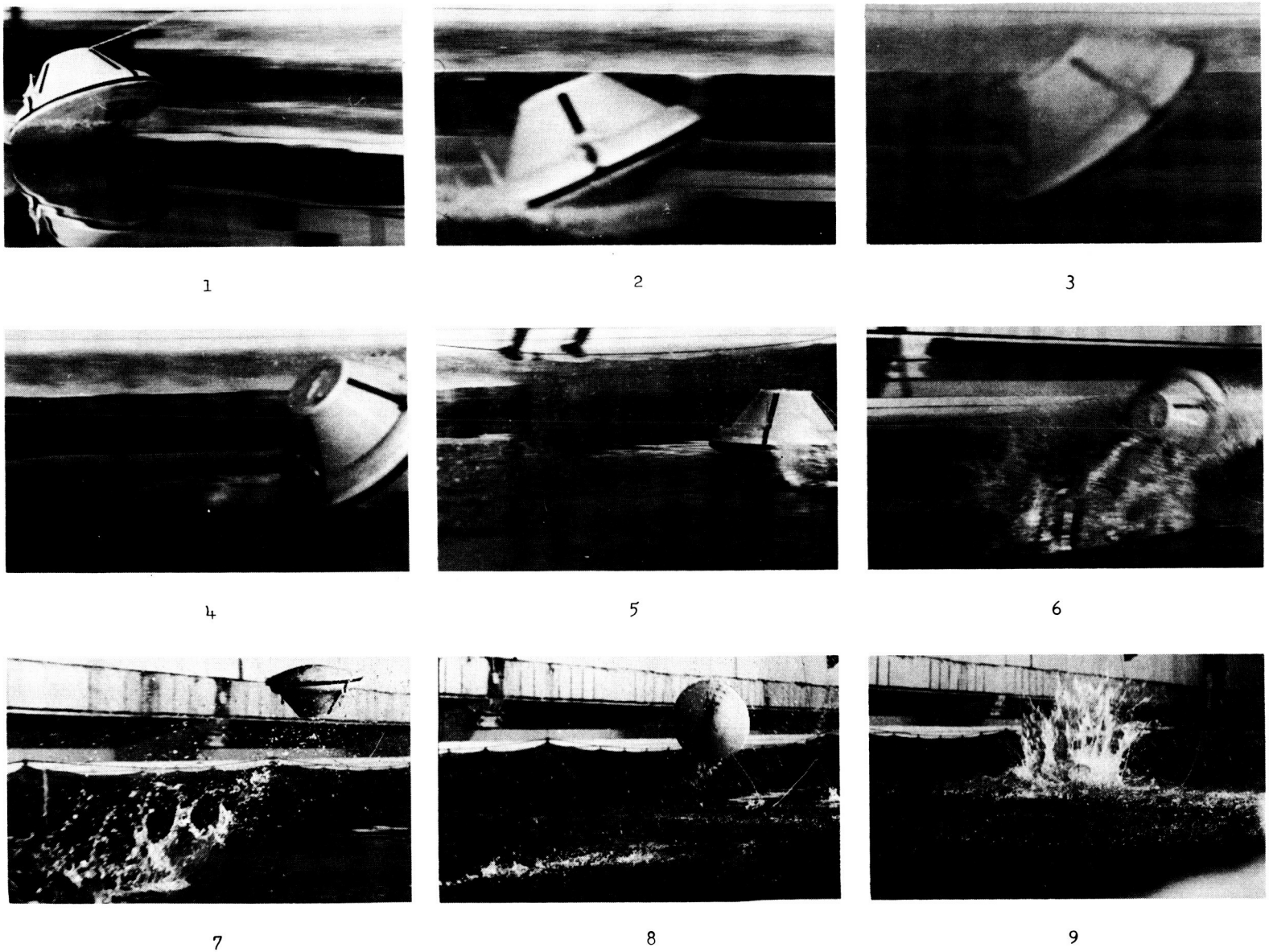

L-63-15

Figure 14.- Sequence photographs of a landing on calm water. Configuration C; horizontal velocity, 130 ft/sec; vertical velocity, 5 ft/sec; landing attitude, 20°.

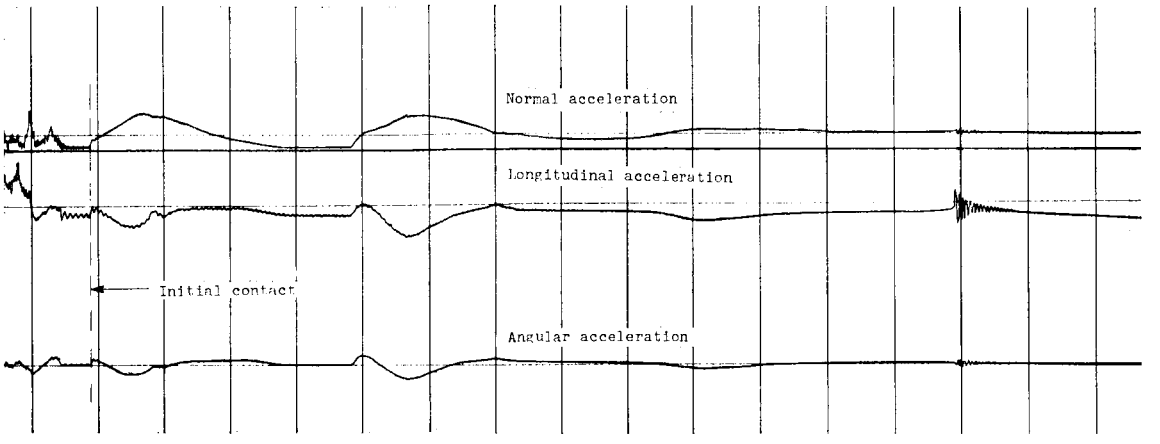

Horizontal velocity 50 ft/sec.

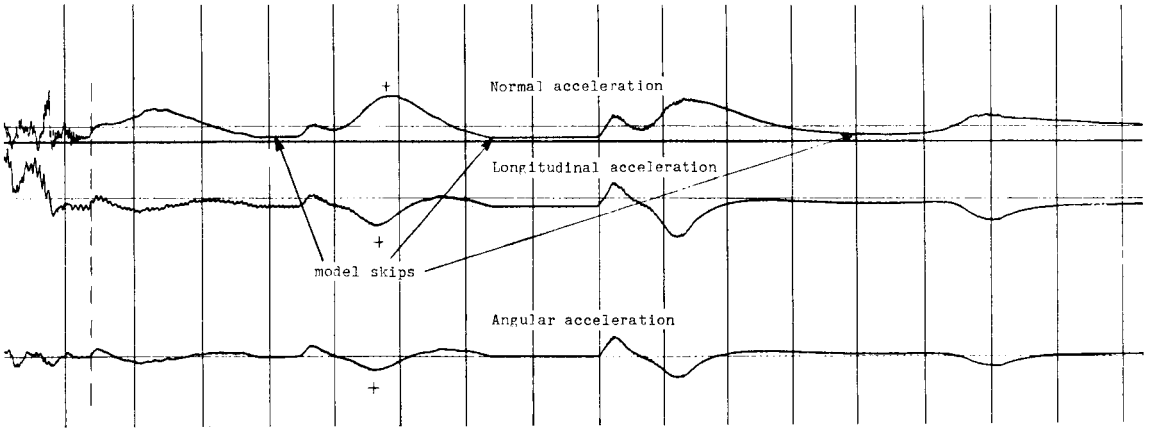

Horizontal velocity 80 ft/sec.

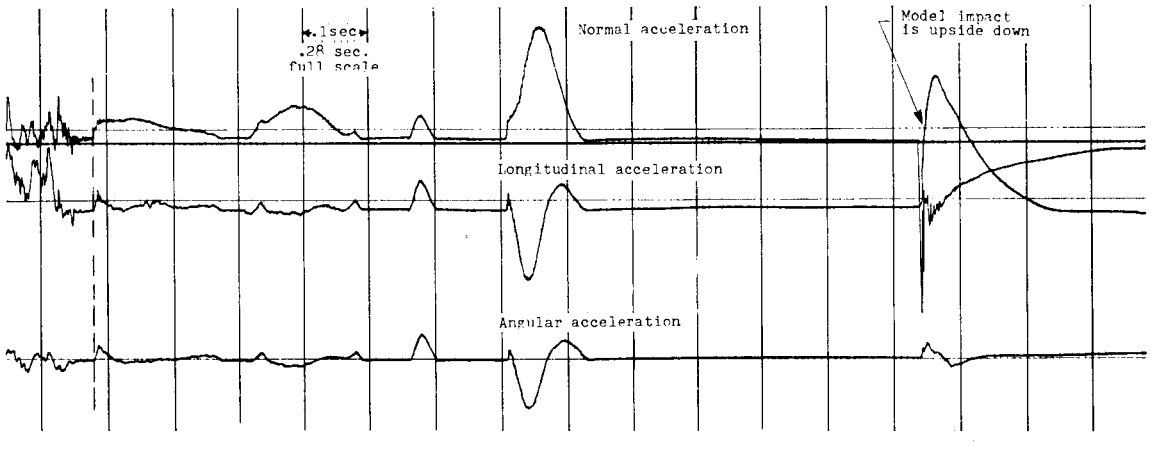

Horizontal velocity 130 ft/sec.

Figure 15.- Typical acceleration time histories of configuration C landing on calm water. Vertical velocity, 5 ft/sec; landing attitude, 20°.

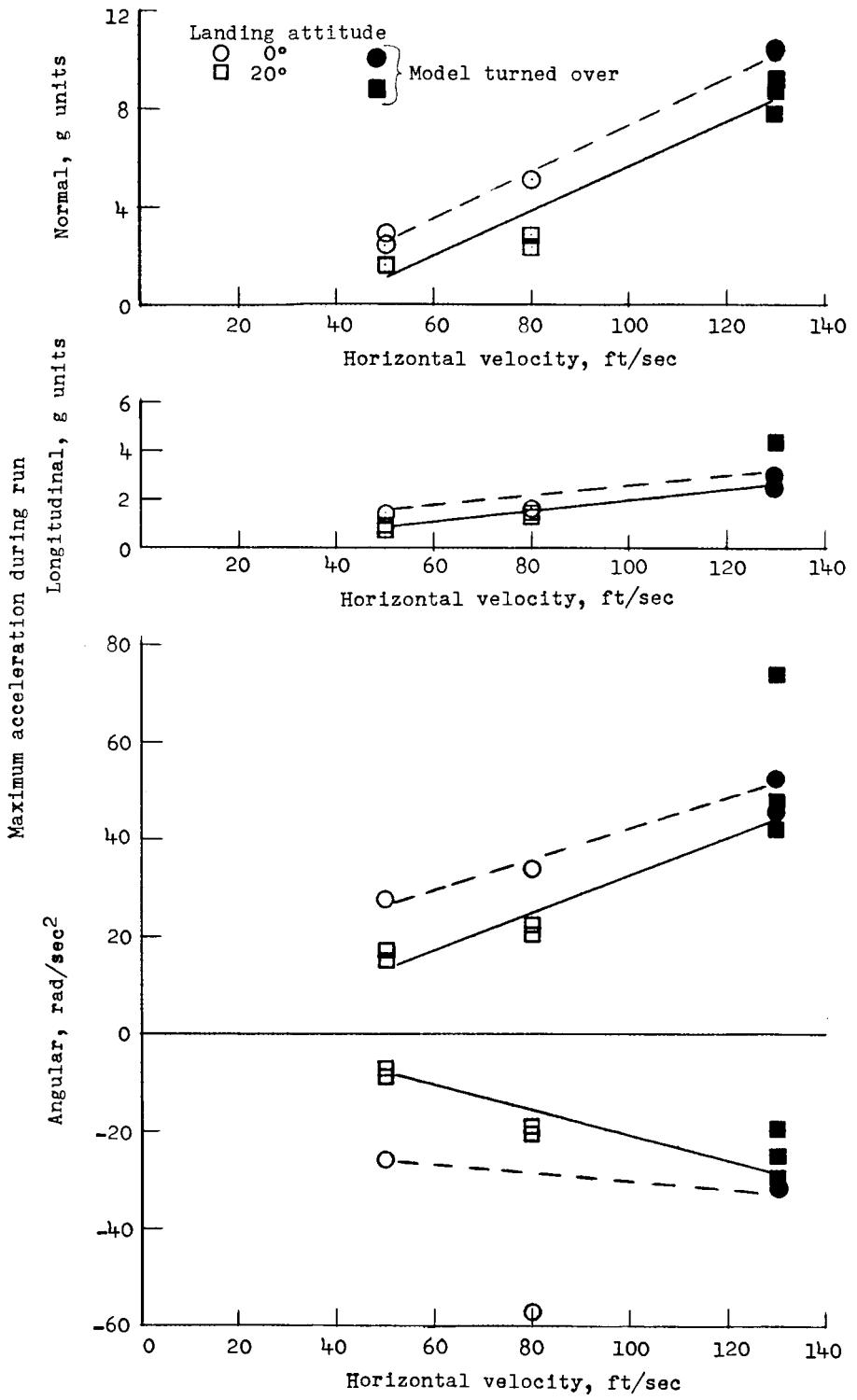

Figure 16.- Maximum acceleration for calm-water landings made with configuration C. Vertical velocity, 5 ft/sec.